Interleukin-17 (IL-17) triggers systemic inflammation, peripheral vascular dysfunction, and related prothrombotic state in a mouse model of Alzheimer's disease

Vellecco, Valentina; Saviano, Anella; Raucci, Federica; Casillo, Gian Marco; Mansour, Adel Abo; Panza, Elisabetta; Mitidieri, Emma; Femminella, Grazia Daniela; Ferrara, Nicola; Cirino, Giuseppe; Sorrentino, Raffaella; Iqbal, Asif Jilani; d'Emmanuele di Villa Bianca, Roberta; Bucci, Mariarosaria; Maione, Francesco

DOI:
10.1016/j.phrs.2022.106595

Document Version
Publisher's PDF, also known as Version of record

Citation for published version (Harvard):
Vellecco, V, Saviano, A, Raucci, F, Casillo, GM, Mansour, AA, Panza, E, Mitidieri, E, Femminella, GD, Ferrara, N, Cirino, G, Sorrentino, R, Iqbal, AJ, d'Emmanuele di Villa Bianca, R, Bucci, M & Maione, F 2023, 'Interleukin-17 (IL-17) triggers systemic inflammation, peripheral vascular dysfunction, and related prothrombotic state in a mouse model of Alzheimer's disease', *Pharmacological Research*, vol. 187, 106595. https://doi.org/10.1016/j.phrs.2022.106595

Pharmacological Research 187 (2023) 106595

Contents lists available at ScienceDirect

Pharmacological Research

journal homepage: www.elsevier.com/locate/yphrs

Interleukin-17 (IL-17) triggers systemic inflammation, peripheral vascular dysfunction, and related prothrombotic state in a mouse model of Alzheimer's disease

Valentina Vellecco [a,1], Anella Saviano [b,1], Federica Raucci [b], Gian Marco Casillo [a], Adel Abo Mansour [c,d], Elisabetta Panza [a], Emma Mitidieri [a], Grazia Daniela Femminella [e], Nicola Ferrara [e,f], Giuseppe Cirino [a], Raffaella Sorrentino [g], Asif Jilani Iqbal [b,c], Roberta d'Emmanuele di Villa Bianca [a], Mariarosaria Bucci [a,*], Francesco Maione [b,**]

[a] Department of Pharmacy, School of Medicine and Surgery, University of Naples Federico II, Via Domenico Montesano 49, 80131 Naples, Italy
[b] ImmunoPharmaLab, Department of Pharmacy, School of Medicine and Surgery, University of Naples Federico II, Via Domenico Montesano 49, 80131 Naples, Italy
[c] Institute of Cardiovascular Sciences (ICVS), College of Medical and Dental Sciences, University of Birmingham, Birmingham B15 2TT, UK
[d] Department of Clinical Laboratory Sciences, College of Applied Medical Sciences, King Khalid University, Abha, Saudi Arabia
[e] Department of Translational Medical Sciences, University of Naples Federico II, 80131 Naples, Italy
[f] Istituti Clinici Scientifici ICS-Maugeri, Telese Terme, BN, Italy
[g] Department of Molecular Medicine and Medical Biotechnologies, School of Medicine, University of Naples, Federico II, Via Pansini, 5, 80131 Naples, Italy

ARTICLE INFO

Keywords:
Alzheimer's disease
IL-17
Immunological perturbance
Systemic inflammation
Vascular dysfunction

ABSTRACT

Alzheimer's disease (AD) is one of the most prevalent forms of neurodegenerative disorders. Previously, we have shown that *in vivo* administration of an IL-17 neutralizing antibody (IL-17Ab) rescues amyloid-β-induced neuroinflammation and memory impairment, demonstrating the pivotal role of IL-17 in AD-derived cognitive deficit. Recently, AD has been recognized as a more intriguing pathology affecting vascular networks and platelet function. However, not much is known about peripheral vascular inflammation and how pro-inflammatory circulating cells/mediators could affect peripheral vessels' function. This study aimed to evaluate whether IL-17Ab treatment could also impact peripheral AD features, such as systemic inflammation, peripheral vascular dysfunction, and related pro-thrombotic state in a non-genetic mouse model of AD. Mice were injected intracerebroventricularly with $A\beta_{1-42}$ peptide (3 μg/3 μl). To evaluate the systemic/peripheral protective profile of IL-17Ab, we used an intranasal administration of IL-17Ab (1 μg/10 μl) at 5, 12, and 19 days after $A\beta_{1-42}$ injection. Circulating Th17/Treg cells and related cyto-chemokines, haematological parameters, vascular/endothelial

Abbreviations: Aβ, amyloid-β Ach acetylcholine; AD, Alzheimer's disease; ADP, Adenosine 5'-diphosphate disodium salt; AUC, area under the curve; BLC, B lymphocyte chemoattractant; CCL-1, chemokine (C-C motif) ligand 1; CNS, central nervous system; COX-, Cyclooxygenase-; Ct, cycle threshold; CTRL, Control; CXCL9, chemokine (C-X-C motif) ligand 9; eNOS, endothelial Nitric Oxide Synthase; GCSF, granulocyte-colony stimulating factor; GM-CSF, granulocyte-macrophage colony-stimulating factor; ICV, intracerebroventricular; IL, interleukin-; IL-17Ab, IL-17A neutralizing antibody; IL-17R, IL-17 Receptor; IN, intranasal; iNOS, inducible Nitric Oxide Synthase; IP-10, interferon gamma-induced protein 10; Iso, isoprenaline; KC, keratinocyte chemoattractant; MCP-1, monocyte-specific cytokine; MCP-5, monocytes chemoattractant protein-5; MIPs, macrophage inflammatory proteins; NIA-AA, U.S. National Institute on Aging-Alzheimer's Association; NO, Nitric Oxide; PBS, phosphate buffered saline; PE, phenylephrine; PRP, platelet-rich plasma; PT, prothrombin time; PTT, partial thromboplastin time; qPCR, quantitative PCR; RANTES, regulated on activation normal T cell expressed and secreted; sICAM, soluble intercellular adhesion molecule-1; TGF-β, transforming growth factor-β; Th, T helper; TIMP-1, tissue inhibitor of metallopeptidase inhibitor-1; TNF-α, tumor necrosis factor-α; Treg, regulatory T cells.

* Correspondence to: Department of Pharmacy, School of Medicine, University of Naples Federico II, Via Domenico Montesano 49, 80131 Naples, Italy.
** Correspondence to: *ImmunoPharmaLab*, Department of Pharmacy, School of Medicine, University of Naples Federico II, Via Domenico Montesano 49, 80131 Naples, Italy.
E-mail addresses: vellecco@unina.it (V. Vellecco), anella.saviano@unina.it (A. Saviano), federica.raucci@unina.it (F. Raucci), gianmarcocasillo@virgilio.it (G.M. Casillo), AMA935@student.bham.ac.uk (A.A. Mansour), e.panza@unina.it (E. Panza), emma.mitidieri@unina.it (E. Mitidieri), graziadaniela.femminella@unina.it (G.D. Femminella), nicferra@unina.it (N. Ferrara), giuseppe.cirino@unina.it (G. Cirino), raffaella.sorrentino@unina.it (R. Sorrentino), a.j.iqbal@bham.ac.uk (A.J. Iqbal), roberta.demmanueledivillabianca@unina.it (R. d'Emmanuele di Villa Bianca), mrbucci@unina.it, mariarosaria.bucci@unina.it (M. Bucci), francesco.maione@unina.it (F. Maione).
[1] Share first authorship.

https://doi.org/10.1016/j.phrs.2022.106595
Received 25 October 2022; Received in revised form 22 November 2022; Accepted 30 November 2022
Available online 5 December 2022

reactivity, platelets and coagulation function in mice were evaluated. IL-17Ab treatment ameliorates the systemic/peripheral inflammation, immunological perturbance, vascular/endothelial impairment and prothrombotic state, suggesting a key role for this cytokine in fostering inflammatory processes that characterize the multifaced aspects of AD.

1. Introduction

Initially identified as an exclusively central nervous system (CNS) disorder, Alzheimer's disease (AD) has been recently recognized to be a more complex pathology affecting the brain vascular network, but also platelet function, and coagulation cascade [1–5]. In this context, it has been proposed that amyloid-β (Aβ)$_{40}$ and Aβ$_{42}$ peptides can interact with several proteins involved in the coagulation cascade, i.e., fibrin/fibrinogen, factor XII, and factor XIIIa, leading to clot formation [6]. Clots derived from Aβ-fibrinogen/fibrin binding display structurally abnormal fibrin clots that are harder to degrade than normal clots and, for this feature, they could represent a potential marker of AD [7]. This condition, coupled with the impaired/overwhelmed clearance of Aβ peptides, contributes to microbleeds and micro- and perivascular distress, known as cerebral amyloid angiopathy (CAA). The impaired perfusion of the neocortex and hippocampus, coupled with a pro-inflammatory microenvironment due to CAA, leads to a slackening of the blood-brain barrier, resulting in the initiation of degenerative processes within the brain tissue [8–10] such as increased recruitment of monocytes and lymphocytes leading to further release of inflammatory factors [11,12]. The increase of fibrin deposition, as well as the levels of fibrinogen-derived peptides, has also been revealed in the brain of humans and mice suffering from AD [13–16]. An aberrant, chronic, primed state of platelets in AD patients has also been reported to contribute to atherothrombosis, formation of leukocytes-platelets aggregates and coagulation abnormalities [10,17]. This evidence reinforces the concept that in AD cerebral vascular dysregulation plays a major role, thereby implying a link between AD and vascular diseases [8]. However, little evidence is available about the potential impact of a pro-neuroinflammatory environment on the peripheral vascular network and if pro-inflammatory circulating cells/mediators could affect peripheral vessels' function.

A large body of experimental reports, including those from our research group, indicate an essential role of T helper (Th) 17 cells and Th17–derived cytokines, such as interleukin (IL)-17 A, IL-21, IL-22, IL-23, granulocyte-macrophage colony-stimulating factor (GM-CSF) in AD onset and progression [18–20]. This evidence is confirmed by the finding that IL-17 is increased in AD [21–23] and that the inhibition of the IL-18/IL-23/IL-17 pathway attenuates AD cognitive deficits [24]. Recently, we have shown that *in vivo* administration of an IL-17 neutralizing antibody (IL-17Ab) rescues amyloid-β-induced neuro-inflammation and memory impairment [18], confirming the pivotal role of IL-17 in AD-derived cognitive deficit. This current study aimed to evaluate whether neutralizing IL-17A (here referred to as IL-17) could also impact the peripheral features of AD, including systemic inflammation, peripheral vascular dysfunction, and related pro-thrombotic state in a non-genetic mouse model of Alzheimer's disease.

2. Materials and methods

2.1. Materials

Recombinant mouse IL-17 A neutralizing antibody (IL-17Ab, cat. MAB421; monoclonal rat IgG$_{2A}$, clone 50104), its related isotype control (cat. MAB006; Control; IgG$_{2A}$, clone 54447) and proteome profiler mouse cytokine Array Kits (cat. ARY006) were purchased from R&D System (Milan, Italy). Aβ$_{1–42}$ (cat. 1428) and Aβ$_{42–1}$ (cat. 3391) amyloid peptides were purchased from Tocris (Milan, Italy). For flow cytometry analysis, the buffers and all conjugated antibodies were obtained from BioLegend (London, UK), Abcam (Milan, Italy) and Origene (Herford, Germany). For clot retraction assay, Microvette® 300 Z (cat. 20.1308) were purchased from Sarstedt (Verona, Italy). Elisa assay for IL-17 (cat. RAB0263), IL-10 (cat. 860.030.096), and TGF-β (cat. 660.050.096) were obtained from Sigma-Aldrich (Milan, Italy), MyBioSource (San Diego, USA) and Diaclone (Besancon Cedex, France), respectively, whereas Aβ$_{1–42}$ (cat. E-EL-M3010) and GM-CSF (cat. MBS2505934) from Elabscience and MyBioSource respectively. Adenosine 5'-diphosphate disodium salt (ADP; CAS: 16178–48–6), trisodium citrate and Tyrode's solution (and all salts for Krebs solution), acetylcholine (Ach; A9101) and isoprenaline (Iso; I5627) were obtained from Sigma-Aldrich (Milan, Italy). Unless otherwise stated, all the other reagents were from BioCell (Milan, Italy).

2.2. Animals

Experimental procedures were carried out in 12-week-old male CD-1 mice in compliance with international and national law and policies and approved by the Italian Ministry of Health. Animal studies were performed in compliance with the ARRIVE guidelines (EU Directive 2010/63/EU for animal experiments, ARRIVE guidelines, and the Basel declaration, including the 3Rs concept) [25,26]. Mice, purchased from Charles River (Milan, Italy), were housed with *ad libitum* access to food and water and maintained on a 12 h light/dark cycle. Experimental study groups were randomized and blinded. All procedures were carried out to minimize the number of animals used (n = 6 per group) and their suffering.

2.3. In vivo animal model and drug administration

Mice were randomly divided into 3 experimental groups: CTRL (Aβ$_{42–1}$ ICV + IgG$_{2A}$ IN), AD (Aβ$_{1–42}$ ICV + IgG$_{2A}$ IN) and IL-17Ab (Aβ$_{1–42}$ ICV + IL-17Ab IN). We used a well-established method for the *in vivo* model consisting of a direct fibrillated Aβ injection, as recently described [27,28]. Method assessment was validated by the simultaneous presence of Aβ monomers and large oligomers (most likely dimers and tetramers), at both 7 and 14 days post model induction, in mice injected with fibrillated Aβ peptide, compared with mice injected with not-fibrillated peptide [18]. Aβ$_{1–42}$ protein was dissolved in phosphate-buffered saline (PBS, 1 μg/μl) in tubes that were sealed and incubated for 1 day at 37 °C to allow peptide assembly state. Anaesthetized mice (mixture of N_2O and O_2 70:30 w/v containing 2% isoflurane) were injected with aggregated Aβ$_{1–42}$ peptide (3 μg/3 μl) or its inactive control peptide Aβ$_{42–1}$ (3 μg/3 μl) into the cerebral ventricle (ICV) at a rate of 1 μl/min, using a microsyringe (10 μl, Hamilton) according to the procedure previously described [27]. The needle was removed after 3 min using three intermediate steps with 1 min interstep delay minimizing backflow. After surgery and Aβ$_{1–42}$ administration, mice were placed on a thermal pad until they recovered from the anaesthesia. All procedures were performed under strictly aseptic conditions. The Hamilton syringe, used for ICV injections, was repeatedly washed with distilled water followed by flushing with 1 mg/ml BSA solution to avoid non-specific binding of peptides to glass. To evaluate the protective profile of IL-17Ab, we used an intranasal (IN) administration route for the antibody IL-17Ab (1 μg/10 μl) and its relative isotype IgG$_{2A}$ (1 μg/10 μl) at 5, 12, and 19 days after Aβ$_{1–42}$ injection. The conditions used for the IN administration of IL-17Ab (volume, body position, and anaesthesia) were based on previously published reports

[18,29]. Mice from the different experimental groups were sacrificed at 7, 14 and 21 days after $A\beta_{1-42}$ protein for subsequent *ex vivo* analysis.

2.4. Flow cytometry

Lymphocytes isolated from whole blood (collected by intracardiac puncture) by Ficoll-Paque Plus density gradient were washed in FACS buffer (PBS containing 1% BSA and 0.02% NaN_2) and directly stained with the following conjugated antibodies: CD3 (1:200, clone 17A2), CD4 (1:200; clone GK1.5; BioLegend), CD8 (1:200; clone 5H10–1; BioLegend), CD25 (1:200; clone 3C7; BioLegend) for 60 min at 4 °C. After washing, cells were fixated, permeabilized, and stained intracellularly with IL-17A (1:200; clone TC11–18H10.1; BioLegend) and FoxP3 antibody (1:200; clone MF-14; BioLegend). Th17 and regulatory T cells (Treg) population were defined as $CD4^+IL\text{-}17^+$ and $CD4^+CD25^+FoxP3^+$ cells respectively [30]. Platelet-rich plasma (PRP) (2×10^5 platelets/μl; see paragraph 2.8 for isolation and characterization) was centrifuged and resuspended in FACS buffer (PBS containing 5% fetal calf serum and 0.02% NaN_2) containing CD16/CD32 FcγIIR-blocking antibody (1:500; clone 2.4G2; eBioscience) for 30 min. Thereafter, cells were incubated for 1 h with the following APC/FITC or PE-conjugated antibodies: CD42b (1:200; SM3032P, Origene), CD62P (1:200; RMP-1, BioLegend), fibrinogen (1:200; ab72925, Abcam) and IL-17 Receptor (IL-17R; CD217; 1:200; W15177A, BioLegend) according to previous reports [31]. T-cells and platelets were successively defined according to the flow cytometry procedure previously described [30,32]. At least 1×10^4 cells were analysed per sample, and positive and negative populations were determined based on the staining obtained with related IgG isotypes [33]. Flow cytometry was performed on BriCyte E6 flow cytometer (Mindray Bio-Medical Electronics, Nanshan, China) using MRFlow and FlowJo software operation [30,34].

2.5. ELISA and ELISA Spot assay

Enzyme-linked immunosorbent assays for $A\beta_{42-1}$ [35], GM-CSF [36], IL-17 [24], IL-10 [37], and transforming growth factor-β (TGF-β) [38] were carried out on plasma as previously described. Briefly, 100 μl of samples, diluted standards, quality controls and dilution buffer (blank) were added to a pre-coated plate with monoclonal anti-$A\beta_{42-1}$, GM-CSF, IL-17, IL-10 or TGF-β for 2 h. After washing, 100 μl of biotin-labelled antibody was added for 1 h. The plate was washed and 100 μl of the streptavidin-HRP conjugate was added and the plate was incubated for a further 30 min period in the dark. The addition of 100 μl of the substrate and stop solution represented the last steps before the reading of absorbance (measured at 450 nm) on a microplate reader. Antigen levels in the samples were determined using a standard curve and expressed as pg/pouch [39,40]. In all described experimental conditions, the cyto-chemokines protein array equal volumes (1.5 ml) of the brain and aortic homogenates and plasma were incubated with the pre-coated proteome profiler array membranes according to the manufacturer's instructions. Dot plots were detected by using the enhanced chemiluminescence detection kit and Image Quant 400 GE Healthcare software (GE Healthcare, Italy) and successively quantified using GS 800 imaging densitometer software (Biorad, Italy) as previously described [41].

2.6. Haematological investigations

Blood was collected via intracardiac puncture to perform haematological investigations of coagulation factors, including prothrombin time (PT; expressed as seconds), partial thromboplastin time (PTT; expressed as seconds) and fibrinogen (expressed as mg/dl), and serological analysis including red blood cells (expressed as 10^6/μl), haematocrit (expressed as %), haemoglobin (expressed as g/dl) and platelets (expressed as 10^3/μl). Haematological investigations were performed by CELL-DYN Sapphire (Abbott SRL; Milan, Italy) [42,43]. All procedures were conducted under strictly aseptic conditions.

2.7. Clot retraction assay

For clot retraction assays, we adopted the protocol proposed by Law and coll. with slight modifications [44]. Briefly, not-anticoagulated blood samples, obtained by intracardiac puncture (300 μl) were transferred into Microvette® 300 Z (Sarstedt, Verona, Italy) containing clotting activator and incubated at room temperature for 2 h. Thereafter, clots were collected and weighed (g), and residual serum volumes (μl) were pipetted as an indirect value of clot reaction [45].

2.8. Platelet aggregation

Blood samples were collected, from all experimental groups, by intracardiac puncture and mixed with trisodium citrate (3.8%, wt/vol). To obtain PRP blood was centrifuged at 200 × *g* [46]. PRP was adjusted with calcium-free Tyrode's solution (NaCl 1.34 mM; KCl 2.9 mM; Na_2HPO_4 0.34 mM; $NaHCO_3$12 mM; HEPES 20 mM; $MgCl_2$ 1 mM; Glucose 0.1%; BSA 0.35%) to obtain 2×10^5 platelets per μl. Platelet aggregation was performed at 37 °C by using Chrono-Log Model 490 optical aggregometer (Chrono-Log, Canada). The aggregation profile was monitored by measuring light transmission changes after ADP stimulation (1, 3 and 10 μM). Results were expressed as % of aggregation and area under the curve (AUC) [31,47].

2.9. Vascular reactivity

Mice from different experimental groups were anaesthetized with enflurane (5%) and then killed in CO_2 chamber (70%). The thoracic aorta was rapidly harvested and cleaned from adherent and connective tissue. Rings of 1–1.5 mm in length were cut from each aorta, placed in organ baths (3.0 ml) filled with oxygenated (95% O_2–5% CO_2) Krebs solution (NaCl 118 mM, KCl 4.7 mM, $MgCl_2$ 1.2 mM, KH_2PO_4 1.2 mM, $CaCl_2$ 2.5 mM, $NaHCO_3$ 25 mM and glucose 10.1 mM) and kept at 37 °C. The rings were connected to an isometric transducer (Fort 25, World Precision Instruments, 2Biological Instruments, Varese, Italy) associated with PowerLab 8/35 (World Precision Instruments, Biological Instruments, Varese, Italy). The rings were initially stretched until a resting tension of 1.0 g and then were allowed to equilibrate for at least 30 min. During this period, when necessary, the tension was adjusted to 1.0 g, and the bath solution was periodically changed [48]. In each set of experiments, rings were firstly challenged with phenylephrine (PE, 1 μM) until the responses were reproducible. Once the plateau was reached, cumulative concentration-response curves to acetylcholine (Ach, 10 nM to 30 μM) and isoprenaline (Iso,10 nM to 30 μM) were performed [49].

2.10. Western blot analysis

Isolated aortas were homogenized in modified RIPA buffer (50-mM Tris-HCl pH 8.0, 150-mM NaCl, 0.5% sodium deoxycholate, 0.1% sodium dodecyl sulfate, 1-mM EDTA, 1% Igepal) containing protease inhibitors cocktail. Protein concentration was determined by Bradford assay using BSA as standard. Denatured proteins (40 μg or 80 μg for iNOS and COX-2 proteins) were separated on 8% sodium dodecyl sulfate-polyacrylamide gels and transferred to a polyvinylidene fluoride membrane. The membranes were blocked by incubation in PBS containing 0.1% v/v Tween 20 and 3% nonfat dried milk (Applichem) for 1 h at room temperature and then incubated overnight at 4 °C with mouse monoclonal anti-endothelial Nitric Oxide (NO) Synthase (eNOS, 1:500, 610297, BD Transduction Laboratories, USA) rabbit polyclonal anti-inducible Nitric Oxide Synthase iNOS (1:1000; D6B6S, Cell Signaling, USA), rabbit polyclonal anti-Cyclooxygenase- (COX-)1 (1:1000; 4841, Cell Signaling, USA) or mouse monoclonal anti-COX-2 (1:1000, 610204, USA) [50]. Membranes were extensively washed in PBS containing 0.1%

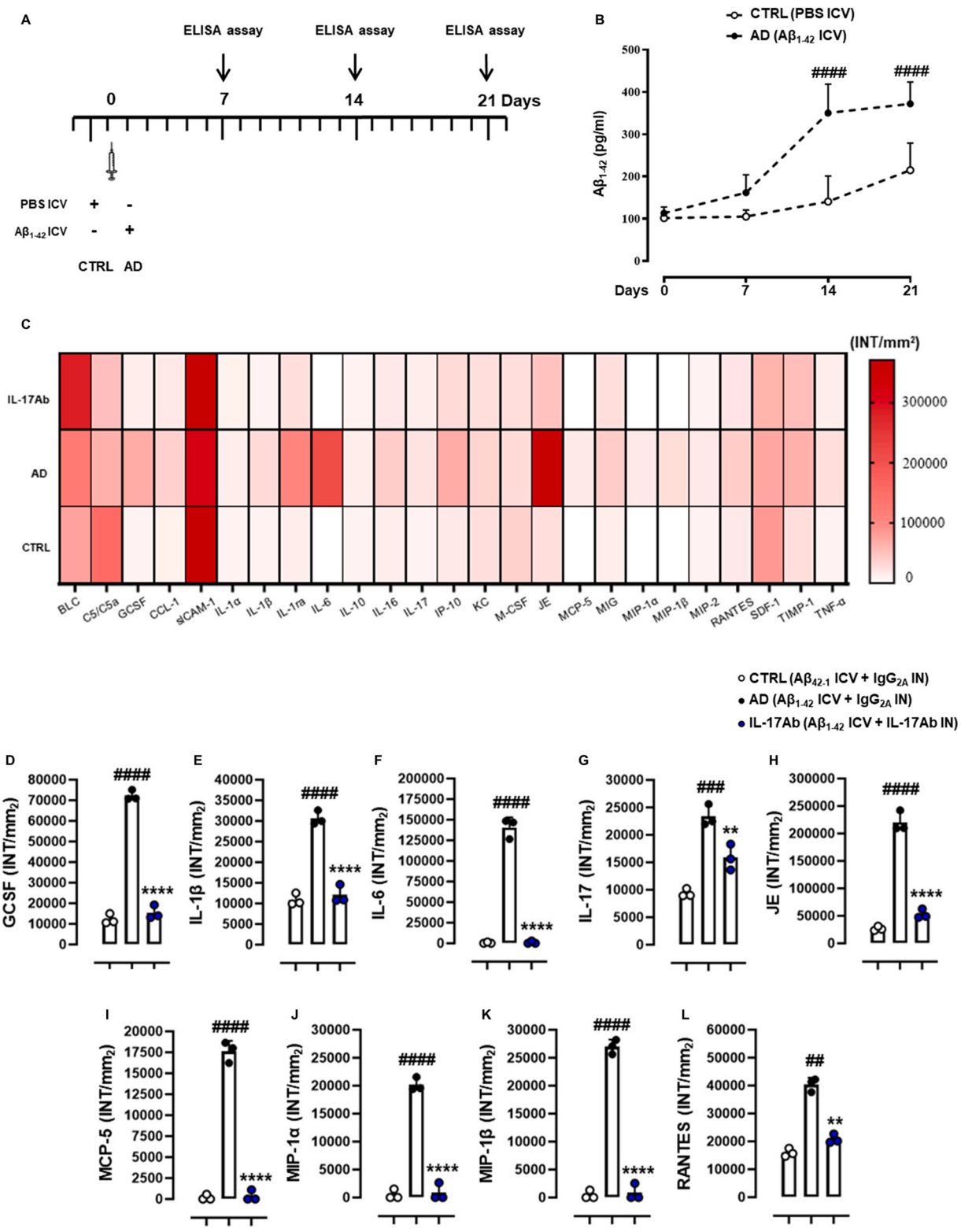

Fig. 1. $A\beta_{1–42}$ drives systemic pro-inflammatory profile and neutralization of IL-17 ameliorates $A\beta_{1–42}$-dependent inflammation. Plasma collected from PBS ICV- and $A\beta_{1–42}$ ICV-injected mice (A) were assayed by ELISA for $A\beta_{1–42}$ (results are expressed as pg/ml) (B). Data are presented as means ± S.D. of n = 6 mice per group. Statistical analysis was conducted by one-way ANOVA followed by Bonferroni's multiple comparisons. $^{\#\#\#\#}P \leq 0.0001$ *vs* CTRL group. Thereafter, plasma from CTRL ($A\beta_{42–1}$ ICV + IgG_{2A} IN), AD ($A\beta_{1–42}$ ICV + IgG_{2A} IN) and IL-17Ab ($A\beta_{1–42}$ ICV + IL-17Ab IN) groups at 21 days' time-point (see Supplementary Fig. 1 for experimental detail) were assayed using a proteome profiler cytokine array. Densitometric analysis is presented as heatmap (C). Values of GCSF (D), IL-1β (E), IL-6 (F), IL-17 (G), JE (H), MCP-5 (I), MIP-1α/β (J-K) and RANTES (L) were extrapolated from heatmap and represented graphically. Data (expressed as INT/mm^2) are presented as means ± S.D. of positive spots of three separate independent experiments run each with n = 6 mice per group pooled. $^{\#\#}P \leq 0.01$, $^{\#\#\#}P \leq 0.001$, $^{\#\#\#\#}P \leq 0.0001$ *vs* CTRL group; $^{**}P \leq 0.01$, $^{****}P \leq 0.0001$ *vs* AD group.

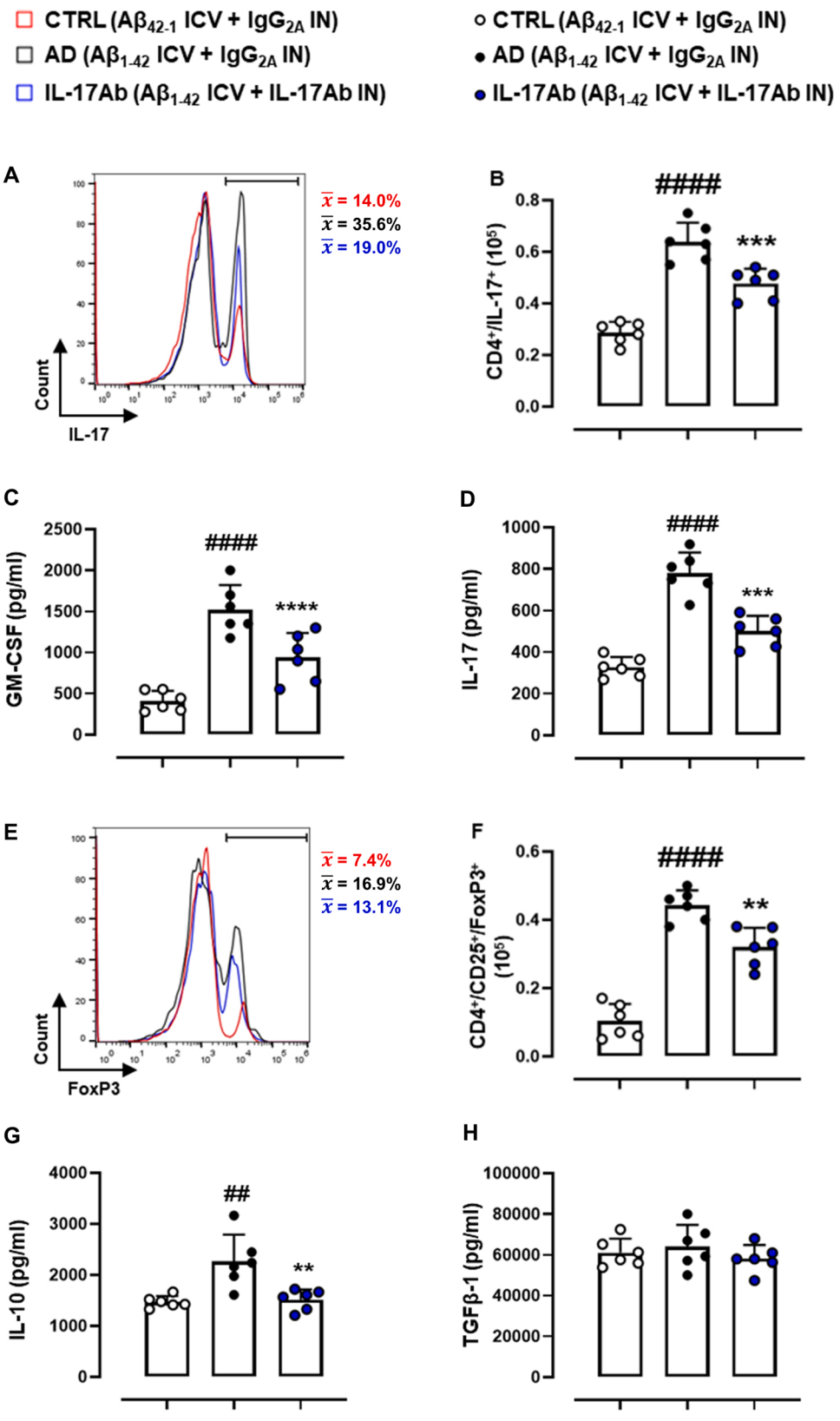

Fig. 2. IL-17 neutralizing antibody blunts Th17/Treg cells increased repertoire. Lymphocytes isolated from whole blood at 21 days' time-point of CTRL ($A\beta_{42-1}$ ICV + IgG_{2A} IN), AD ($A\beta_{1-42}$ ICV + IgG_{2A} IN) and IL-17Ab ($A\beta_{1-42}$ ICV + IL-17Ab IN) groups by Ficoll-Paque Plus gradient method were gated in their totality and singlet before the identification of $CD4^+$/$IL\text{-}17^+$ (A, Th17 population) and $CD4^+$/$CD25^+$/$FoxP3^+$ (E, Treg population). Histograms indicate the total positive populations (expressed as $x10^5$ and calculated from means of % of positive cells), in the different experimental conditions (B, F). FACS pictures are representative of three independent experiments with similar results. Thereafter, plasma collected in the same experimental conditions were assayed by ELISA for GM-CSF (C), IL-17 (D), IL-10 (G) and TGFβ-1 (H) (expressed as pg/ml). Data are presented as means ± S.D. of n = 6 mice per group. Statistical analysis was conducted by one-way ANOVA followed by Bonferroni's multiple comparisons. $^{\#\#}P \leq 0.01$, $^{\#\#\#\#}P \leq 0.0001$ *vs* CTRL group; $^{**}P \leq 0.01$, $^{***}P \leq 0.001$, $^{****}P \leq 0.0001$ *vs* AD group.

v/v Tween 20 before incubation with horseradish peroxidase-conjugated secondary antibody for 2 h at room temperature. Following incubation, membranes were washed and developed using Chemidoc (Bio-Rad, Italy). The target protein band intensity was normalized over the intensity of the housekeeping protein β-actin (1:5000, A4700 Clone: AC40, Sigma-Aldrich, Italy) [51].

2.11. RNA extraction and quantitative PCR (qPCR)

Total RNA was isolated from the mouse aorta by use of the TRI-

Reagent (Sigma-Aldrich, Milan, Italy), according to the manufacturer's instructions, and quantized to the NanoDrop. The final preparation of RNA was considered DNA- and protein-free if the ratio between readings at 260/280 nm was ≥ 1.7. Isolated mRNA was reverse transcribed by the use of iScript Reverse Transcription Supermix for RTqPCR (Bio-Rad, Milan, Italy). Quantitative PCR (qPCR) was carried out in a real-time PCR system CFX96 (Bio-Rad) using the SsoAdvanced SYBR Green supermix (cat. n. 1725274, Bio-Rad Milan Italy) detection technique. qPCR was performed on independent biological samples ≥ 4–5 for each experimental group. Each sample was amplified simultaneously in triplicate in a one-assay run with a non-template control blank for each primer pair to control for contamination or primer-dimer formation, and the cycle threshold (Ct) value for each experimental group was determined. The housekeeping gene (actin) was used to normalize the Ct values, using the 2^− ΔCt formula; differences in mRNA content between groups were expressed as 2^− ΔΔCt [52]. Primers Sequence (5'->3'): IL-17A fw TCAGCGTGTCCAAACACTGAG rev CGCCAAGGGAGTTAAAGACTT; IL-17RA fw AGTGTTTCCTCTACCCAGCAC rev GAAAACCGCCACCGCTTAC; IL-17RC fw TTCTGCGGTATTTGACTGTTTCG rev GTCCCGGACTTCAAGACCC; actin fw GGCTGTATTCCCCTCCATCG rev CCAGTTGGTAACAATGCCATGT [53].

2.12. Data and analysis

In this study, statistical analysis complies with the recommendations on experimental design and analysis in pharmacology [54] and data sharing and presentation in preclinical pharmacology [55,56]. All data presented as means ± S.D. were analysed using Student's t-test (two groups), one-way or two-way ANOVA followed by Bonferroni's and Tuckey's for multiple comparison tests (more than two groups). GraphPad Prism 8.0 software (San Diego, CA, USA) was used for analysis. Differences between means were considered statistically significant when $P \leq 0.05$ was achieved. The sample size was chosen to ensure alpha 0.05 and power 0.8. Animal weight was used for randomization and group allocation to reduce unwanted sources of variations by data normalization. *In vivo* and *in vitro* studies were carried out to generate groups of equal size (n = 4–6 of independent values), using randomization and blinded analysis. The figure legends specify data and statistical tests for each experiment.

3. Results and discussion

3.1. $A\beta_{1-42}$ drives systemic pro-inflammatory profile, and neutralization of IL-17 ameliorates $A\beta_{1-42}$-dependent inflammation

Increased plasma levels of $A\beta_{1-42}$ have been detected in both preclinical investigations and clinical studies of AD [35,57]. Therefore, to verify if, in a non-genetic mouse model of AD, ICV administration of fibrillated $A\beta_{1-42}$ could affect the systemic levels of Aβ fragments, we monitored $A\beta_{1-42}$ plasmatic concentration following 7, 14 and 21days post $A\beta_{1-42}$ ICV by ELISA (Fig. 1A). As shown in Fig. 1B, $A\beta_{1-42}$ higher levels were found as early as 7 days, followed by a further significant increase at the late stage (14–21 days).

Recent literature proposes multiple mechanisms contributing to AD onset and progression linked to high levels of circulating $A\beta_{1-42}$, which include systemic inflammation, immune dysregulation (related to Th17/Treg ratio), and vascular dysfunction [58–60]. T lymphocytes are particularly involved in the inflammatory/immunological response associated with AD (and with the "release" of $A\beta_{1-42}$), and activated T-cells can easily cross the blood-brain barrier contributing to the ongoing inflammatory repertoire and disease pathogenesis and progression [18]. The current experimental findings extend upon our previous findings showing that IL-17 is a detrimental factor for AD, where this particular cytokine (especially by its selective expression in the hippocampus and prefrontal cortex) could represent a key factor for the "self-amplifying" neuro-inflammatory onset typically associated with Aβ-related disease. Indeed, in the revised criteria for AD, by the U.S. National Institute on Aging-Alzheimer's Association (NIA-AA) workgroups, the disease's diagnosis is no longer "merely" based on clinical examination and neuropsychiatric tests but also includes the detection of Aβ peptides [61] add circulating pro-inflammatory mediators and soluble factors. In particular, tumor necrosis factor-α (TNF-α) [62], IL-1α/β [63], IL-6 [64], IL-7 [65], IL-15 [66] and IL-18 [67], but also IL-17 [22] and IL-10 [68] have been identified as "critical factors/-markers" for AD. To assess if our murine model of AD could recapitulate the systemic peripheral features indicated by NIA-AA, we used an unbiased approach (pre-made protein array) based on profiling cyto-chemokines detected in both total brain homogenates and plasma. Mice were divided into 3 experimental groups: CTRL ($A\beta_{42-1}$ ICV + IgG_{2A} IN), AD ($A\beta_{1-42}$ ICV + IgG_{2A} IN) and IL-17Ab ($A\beta_{1-42}$ ICV + IL-17Ab IN) (see Supplementary Fig. 1). As shown in the heat map in Fig. 1C, at the peak of amyloidosis (day 21) AD group displayed a marked increase in plasmatic levels of several cyto-chemokines and soluble factors such as granulocyte-colony stimulating factor (GCSF), chemokine (C-C motif) ligand 1 (CCL-1), IL-1β/ra, IL-6, IL-16, IL-17, interferon gamma-induced protein 10 (IP-10), monocyte-specific cytokine (MCP-1, also known as JE), monocytes chemoattractant protein-5 (MCP-5), chemokine (C-X-C motif) ligand 9 (CXCL9 also known as MIG), macrophage inflammatory protein (MIP)− 1α, and − 1β, normal T lymphocyte chemotactic cytokine (regulated on activation, normal T cell expressed and secreted; RANTES), compared to CTRL group. Interestingly, in the IL-17Ab group, we detected not only a significant reduction in the aforementioned factors (Fig. 1C) but also a reversion to basal values of GCSF, IL-1β, IL-6, IL-17, JE, MCP-5, MIP1α/β and RANTES (Fig. 1D-L). A not significant trend was observed in the brain (Supplementary Fig. 2) and plasma (Supplementary Fig. 3) after 7 and 14 days post $A\beta_{1-42}$ ICV injection.

Thus, neutralization of IL-17 exerts a beneficial action on the brain, protecting from $A\beta_{1-42}$-dependent pro-inflammatory cyto-chemokines production involved in systemic/peripheral inflammation as supported by a large body of experimental reports, including those from our research group [18].

3.2. IL-17 neutralizing antibody blunts Th17/Treg cells increased repertoire

Treg cells are of fundamental importance in modulating the relative balance between inflammation and systemic immune tolerance in AD [68,69]. To correlate $A\beta_{1-42}$ ICV with the development of a specific circulating Th profile, we isolated lymphocytes from all groups at 7, 14 and 21 days and stained isolated cells for CD4/IL-17 and CD4/CD25/FoxP3 for the identification of Th17 and Treg population, respectively (gating strategy reported in Supplementary Fig. 4) [30,70].

At the peak of "amyloidosis" (day 21) AD group displayed a marked increase in $Th17^+$ cells compared to CTRL (Fig. 2A-B). This cellular phenotype was associated with a significant increase in GM-CSF (Fig. 2C) and IL-17 (Fig. 2D). Treatment with IL-17Ab significantly reduced both the number of circulating $CD4^+/IL\text{-}17^+$ cells (Fig. 2B) and the levels of GM-CSF (Fig. 2C) and IL-17 (Fig. 2D). $A\beta_{1-42}$ ICV was also associated with a significant increase of both circulating $CD4^+/CD25^+/FoxP3^+$ (Treg) cells (Fig. 2E-F) and IL-10 production (Fig. 2G). Notably, following the treatment with the IL-17Ab, we observed a significant reduction in Treg profile (Fig. 2F) and IL-10 (Fig. 2G). Conversely, no significant differences were found for TGF-β (Fig. 2H). At the earlier stage of $A\beta_{1-42}$ ICV injection (7 and 14 days), IL-17Ab did not significantly affect either Th17 (Supplementary Fig. 5) or Treg (Supplementary Fig. 6) expansion and activation, suggesting that the beneficial effect exerted by IL-17Ab is reached through the cumulative dose administered. Th17/Treg cellular analysis was strengthened by a lower percentage of positive cells found in all the staining for the isotype control antibodies (Supplementary Fig. 7) and by no significant changes on circulating $CD3^+$ and $CD8^+$ cells between AD and IL-17Ab group

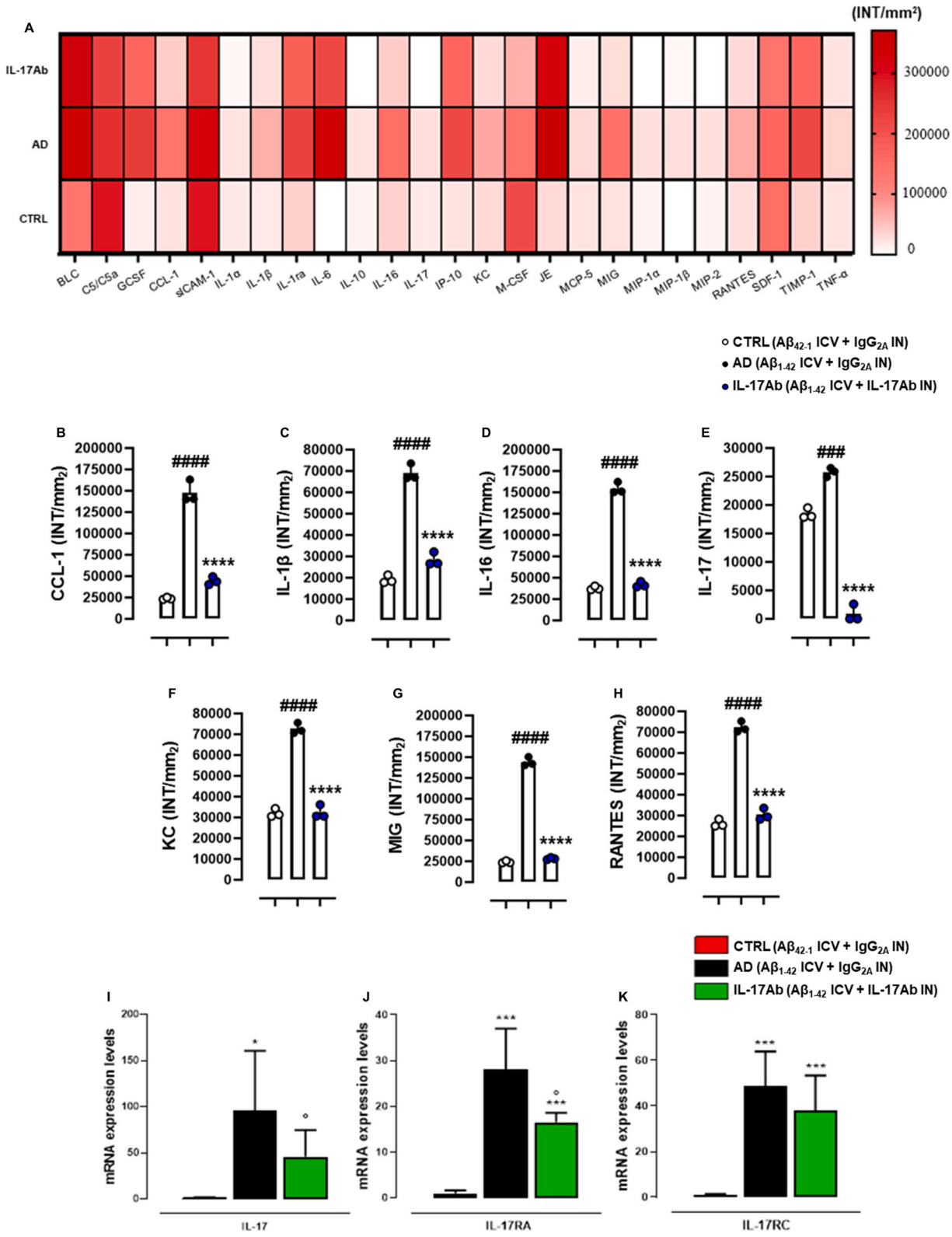

Fig. 3. Neutralization of IL-17 ameliorates AD-related vascular inflammation. Homogenates obtained from aorta (harvested at 21 days) of CTRL ($A\beta_{42-1}$ ICV + IgG_{2A} IN), AD ($A\beta_{1-42}$ ICV + IgG_{2A} IN) and IL-17Ab ($A\beta_{1-42}$ ICV + IL-17Ab IN) groups were assayed using a proteome profiler cytokine array. Densitometric analysis is presented as heatmap (A). Thereafter, values of CCL-1 (B), IL-1β (C), IL-16 (D), IL-17 (E), KC (F), MIG (G) and RANTES (H) were extrapolated from heatmap and represented graphically. Data (expressed as INT/mm^2) are presented as means ± S.D. of positive spots of three separate independent experiments run each with n = 6 mice per group pooled. $^{\#\#\#}P \leq 0.001$, $^{\#\#\#\#}P \leq 0.0001$ *vs* CTRL group; $^{****}P \leq 0.0001$ *vs* AD group (B-H). mRNA expression of IL-17 (I), IL-17RA (J) and IL-17RC (K) in aorta from CTRL, AD and IL-17Ab groups at 21 days' time points was evaluated. Data were expressed as mean ± S.D. of n = 4 mice per group. Statistical analysis was conducted by one-way ANOVA followed by Tukey's for multiple comparisons. $^{*}P \leq 0.05$, $^{***}P \leq 0.001$ *vs* CTRL group; $^{\circ}P \leq 0.05$ *vs* AD group.

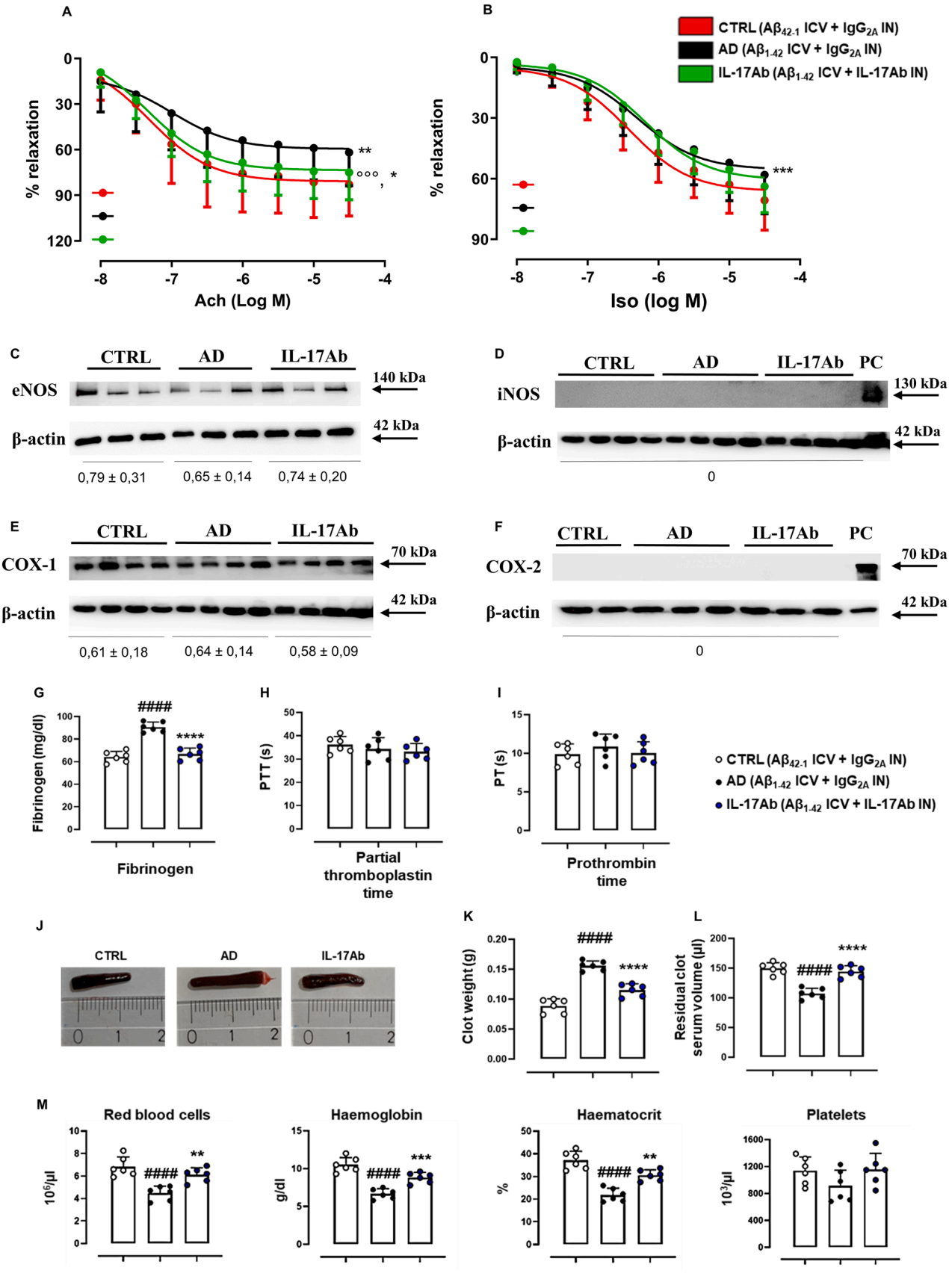

(caption on next page)

Fig. 4. Neutralization of IL-17 affects endothelial reactivity and reduces clot formation. Concentration–response curves of acetylcholine (A; 10 nM to 30 μM) and isoprenaline (B; 10 nM to 30 μM) on a stable tone of phenylephrine (1 μM) on aorta rings harvested at 21 days in all experimental conditions, were performed. Values are expressed as means ± S.D. of n = 6 mice per group and expressed as % relaxation. Statistical analysis was conducted by two-way ANOVA followed by Bonferroni's for multiple comparisons.*P ≤ 0.05, **P ≤ 0.01, ***P ≤ 0.001 *vs* CTRL group; °°°P ≤ 0.001 *vs* AD group (A-B). Aorta ring homogenates, harvested at 21 days' time-point in all experimental conditions, were assayed by western blot for eNOS (C), iNOS (D), COX-1 (E), and COX-2 (F). Western blot imagines are representative of three separate experiments with similar results. Values of cumulative densitometric values, reported at the bottom of related figures, are expressed as OD Ratio with actin. Values are presented as means ± S.D. of three separate independent experiments run each with n = 6 mice per group pooled. Statistical analysis was conducted by one-way ANOVA followed by Bonferroni's for multiple comparisons. Haematological investigations were assessed on blood samples at 21 days post model induction on CTRL ($A\beta_{42-1}$ ICV + IgG_{2A} IN), AD ($A\beta_{1-42}$ ICV + IgG_{2A} IN) and IL-17Ab ($A\beta_{1-42}$ ICV + IL-17Ab IN) groups. The effect on the coagulation process and fibrinolytic activity were determined by measuring fibrinogen (expressed as mg/dl) (G), PTT (expressed as s) (H), and PT (expressed as s) (I). The effect of IL-17Ab on clot formation was evaluated, macroscopically, by a clot retraction assay (J), and quantified measuring their weights (expressed as g) (K), and their residual serum volumes (expressed as μl) (L). Finally, haematological indexes related to red blood cells (expressed as 10^6/μl), haemoglobin (expressed as g/dl), haematocrit (expressed as %), and platelets (expressed as 10^3/μl) were evaluated (M). Data are presented as means ± S.D. of n = 6 mice per group. Statistical analysis was conducted by one-way ANOVA followed by Bonferroni's for multiple comparisons. ####P ≤ 0.0001 *vs* CTRL group; * *P ≤ 0.01, ***P ≤ 0.001, ****P ≤ 0.0001 *vs* AD group (G-M).

(Supplementary Fig. 8). According to relevant literature, we have: i) confirmed that the onset and progression of the disease are associated with increased circulating levels of Th17 and Treg; ii) demonstrated that treatment with IL-17Ab modulates the inflammatory response by restoring Th17/Treg ratio repertoire. Thus, in this AD mouse model, IL-17 plays a pivotal role not only in Th17-pathogenic activity but also in the Treg cells-driven immunological tolerance.

3.3. Neutralization of IL-17 ameliorates AD-related vascular inflammation and reduces clot formation

To assess whether the systemic inflammatory state was also correlated to peripheral vascular inflammation and dysfunction, we performed a cyto-chemokines analysis on aorta homogenates at 7, 14 and 21 days post $A\beta_{1-42}$ ICV injection. A deep alteration in the pattern of inflammatory factors was evident in vascular tissues. Indeed, as shown in the heat map in Fig. 3A, at the 21-day time-point, the AD group displayed a marked increase of B lymphocyte chemoattractant (BLC), GCSF, CCL-1, soluble intercellular adhesion molecule-1 (sICAM), IL-1β/ra, IL-6, IL-16, IL-17, IP-10, keratinocyte chemoattractant (KC), JE, MIG, RANTES and tissue inhibitor of metallopeptidase inhibitor-1 (TIMP-1) compared to CTRL. Following IL-17Ab treatment, there was a marked reduction in the factors mentioned previously (Fig. 3A) and a reversion to basal levels of CCL-1, IL-1β, IL-16, IL-17, KC, MIG and RANTES (Fig. 3B-H). Similarly, to immunological assessment, no significant differences between AD and IL-17Ab groups were revealed after 7 and 14 days (Supplementary Fig. 9). To investigate if such a pro-inflammatory profile was related to the activation of IL-17 signalling, we evaluated the transcript expression of IL-17 and its primary receptors (IL-17RA and IL-17RC) in aorta samples harvested on day 21. As shown in Fig. 3I-K, in AD, a significant increase of all three genes was observed compared to CTRL. IL-17Ab treatment reduced the mRNA expression of both IL-17 (Fig. 3I) and IL-17RA (Fig. 3J) whilst no significant differences were found for the accessory receptor IL-17RC (Fig. 3K). All these data strongly imply a key role for IL-17 (mainly produced by $Th17^+$ cells) signalling in orchestrating and sustaining the peripheral vascular inflammation associated with AD.

Does this inflammatory environment affect vascular function? The experiments performed using isolated aorta rings indicated that in AD mice there is a significant reduction of both Ach- and Iso-induced vasorelaxation compared to CTRL group (Fig. 4A-B respectively). The lack of effect of the IL-17Ab treatment on the major enzymes involved in vessel reactivity, namely endothelial nitric oxide synthase (eNOS, Fig. 4C), inducible nitric oxide synthase (iNOS, Fig. 4D), cyclooxygenase 1 (COX-1, Fig. 4E) and cyclooxygenase 2 (COX-2, Fig. 4F) suggested that IL17/IL17R pathway does not modulate these canonical vascular enzymes. When tissues were incubated with the IL-17Ab, Ach-induced vascular response was rescued (Fig. 4A-B). Since Ach-induced vasodilatation is exclusively endothelium-dependent, this result indicates a targeted action on the endothelium. Conversely, the lack of effect on Iso implies a lack of action on smooth muscle cells [48, 71–73].

It is well-established that the endothelium is the first link between inflammation and coagulation. Indeed, dysfunctional endothelium represents not only the interface between plasmatic inflammatory mediators/cells and vessels but also the surface where molecules involved in both coagulation and the development of inflammation are exposed [74]. Recent studies show that during AD onset and progression, the activation of several "latent and silent" coagulation factors takes place [8,75]. This concept is in line with the endothelium protective effect of the IL-17Ab above discussed. As reported in Fig. 4G, IL-17Ab treatment prevented the fibrinogen increase observed in the AD group without affecting PTT (Fig. 4H) or PT (Fig. 4I). To verify the relevance of increased fibrinogen on clot formation, we next analysed the clot retraction in all groups. Clot morphology (Fig. 4J), clot weight (Fig. 4K) and residual clot serum volumes (Fig. 4L) changes were all significantly reduced by IL-17Ab treatment. In the AD group, there was also a significant decrease in red blood cells (day 21, expressed as 10^6/μl), haemoglobin (day 14 and 21, expressed as g/dl), and haematocrit (day 21, expressed as %) (Fig. 4M).

This data is in line with previous reports that show circulating abnormalities in AD patients [1,2]. IL-17Ab treatment reverted this formula to physiological values (Supplementary Fig. 10), whilst no significant variances were observed for platelets among groups (expressed as 10^3/μl) in all experimental time-points. Taken together, all these data depict a peripheral vascular dysfunction in which the endothelium impairment leads to an inflammatory/pro-thrombotic state. The beneficial effects of IL-17Ab unveil the main role of IL-17 in developing these phenomena.

3.4. Neutralization of IL-17 modulates AD-related platelets activation and pro-aggregative state

The lack of effect on platelet counts, combined with the beneficial effect of IL-17Ab on clot formation, suggested a possible modulation of platelet function and activation by IL-17. This hypothesis relies on the following evidence: i) a functional IL-17 receptor is expressed on both murine and human platelets [31]; ii) increasing clinical evidence shows that enhanced platelet activation is a feature of AD-related vascular dysfunction [76]. Here, the platelet-activating profile examined by using flow cytometry and samples collected on day 21 demonstrate that in AD samples there is a significant increase in fibrinogen and CD62P expression as compared to CTRL group (Fig. 5). IL-17Ab treatment selectively reverted the expression of fibrinogen (Fig. 5D), leaving unchanged the level of CD62P (Fig. 5E). $CD42b^+$ cells (a specific marker of platelets), were gated for expression of fibrinogen-binding sites on the αIIbβ3 integrin, CD62P and IL-17R (gating strategy reported in Supplementary Fig. 11) according to the protocol described previously [31]. A possible direct effect of IL-17 on its receptor was ruled out by the lack of significant changes in IL-17R extra-cellular expression among the experimental groups (Fig. 5F). Reported values were strengthened by a low

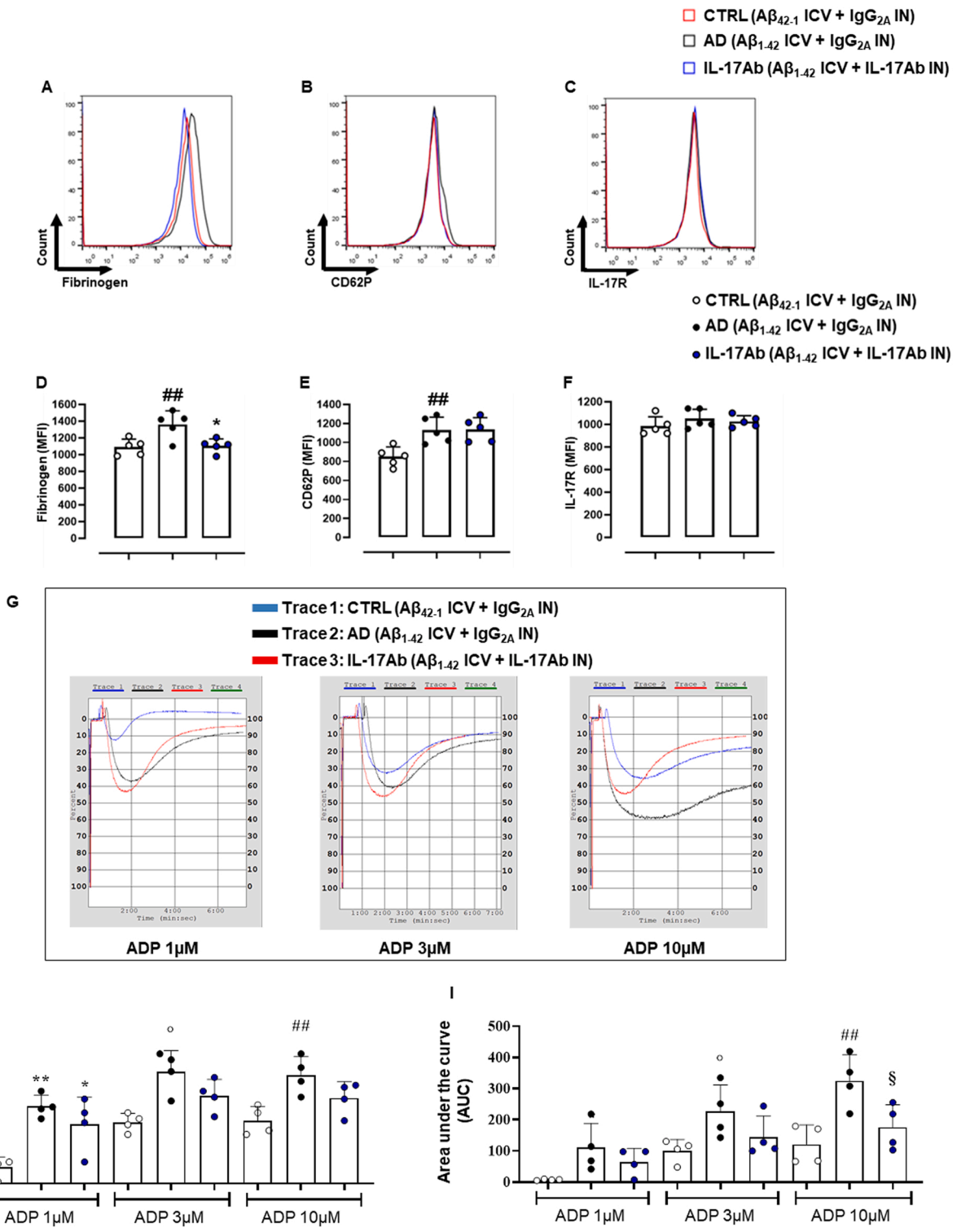

Fig. 5. Neutralization of IL-17 modulates AD-related platelets activation and pro-aggregative state. PRP, isolated from whole blood at 21 days' time-point for CTRL ($A\beta_{42-1}$ ICV + IgG_{2A} IN), AD ($A\beta_{1-42}$ ICV + IgG_{2A} IN) and IL-17Ab ($A\beta_{1-42}$ ICV + IL-17Ab IN) group, was firstly gated for CD42b before the identification of Fibrinogen^{+} (A), CD62P^{+} (B), and IL-17 Receptor^{+} (C). Histograms indicate the total positive populations (expressed as Mean Fluorescent Intensity, MIF) (D-F), in the different experimental conditions. FACS pictures are representative of three independent experiments with similar results. Data are presented as means ± S.D. of n = 5 mice per group. Statistical analysis was conducted by one-way ANOVA followed by Bonferroni's for multiple comparisons. $^{\#\#}P \leq 0.01$ *vs* CTRL group; $^{*}P \leq 0.05$ *vs* AD group. Platelet functionality was evaluated at 21-day time-point in all experimental conditions. Representative tracers of ADP-induced aggregation at 1, 3 and 10 μM (G). Results were reported as % of aggregation (H) and AUC (I). Data are expressed as mean ± S.D. of n = 4 mice per group. Statistical analysis was conducted by one-way ANOVA followed by Bonferroni's for multiple comparisons. $^{*}P \leq 0.05$, $^{**}P \leq 0.01$ *vs* its own CTRL group; $^{\circ}P \leq 0.05$ *vs* its own CTRL group; $^{\#\#}P \leq 0.01$ *vs* its own CTRL group; §P ≤ 0.05 *vs* its own AD group.

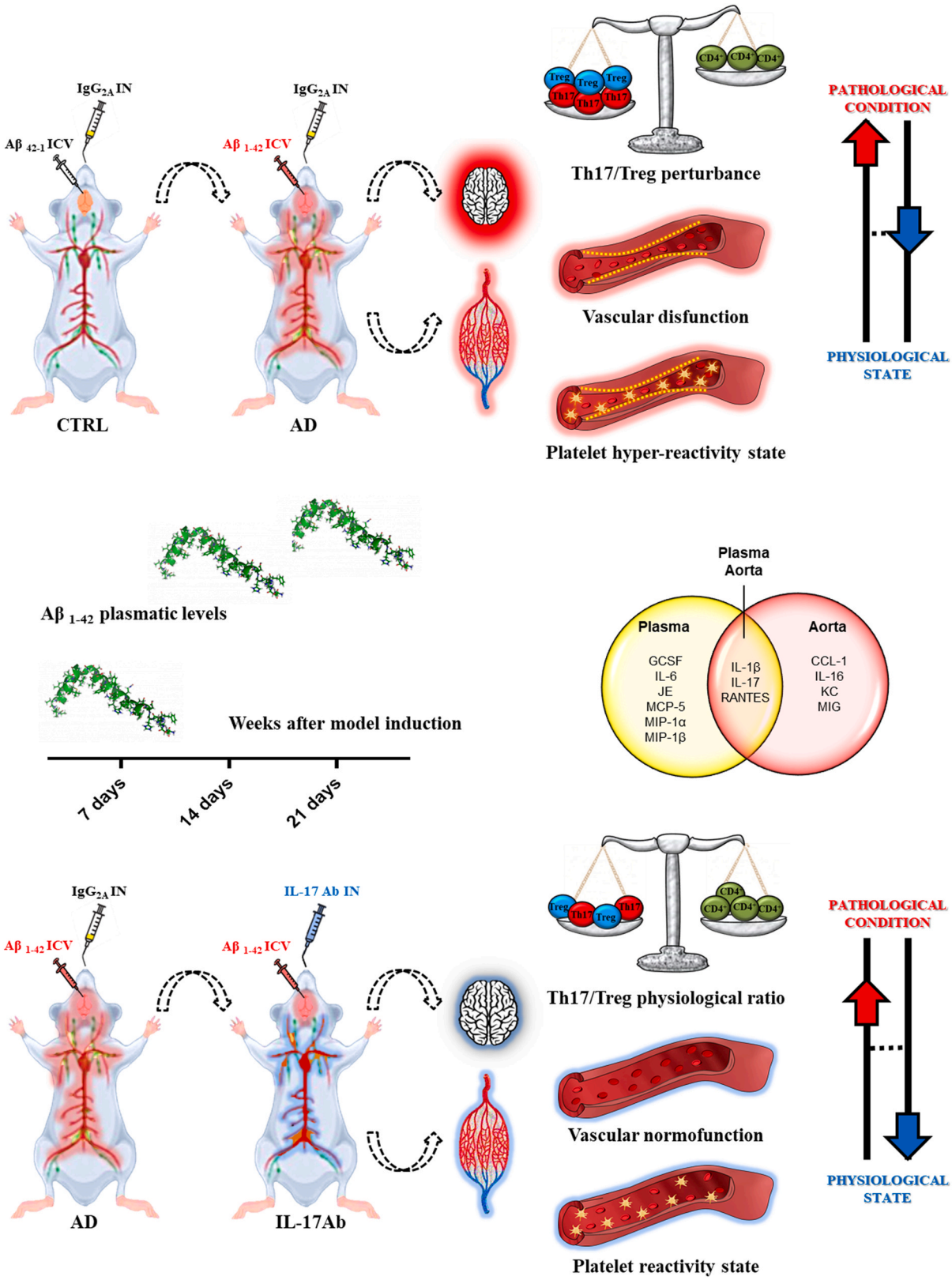

Fig. 6. Neutralization of interleukin-17 (IL-17) modulates systemic inflammation, peripheral vascular dysfunction, and related prothrombotic state in Alzheimer's disease. Our findings propose that AD is strictly associated with systemic inflammation and peripheral vascular dysfunction. Intracerebroventricular (ICV) administration of $A\beta_{1-42}$ in mice (upper left panel) is paralleled accompanying to a plasmatic increase of fibrillated peptide after $A\beta_{1-42}$ ICV injection (middle left panel). $A\beta_{1-42,}$ inducing neuro-inflammation, promotes an unbalance Th17/Treg ratio that concomitantly fuels, mainly through IL-17, a vascular/endothelial inflammation and platelet hyper-reactivity state (upper right panel). The Venn diagram (shown in the middle right panel) highlights the pro-inflammatory mediators (IL-17 related) "normally" upregulated in the later stage (21 days) of the disease. Our findings also revealed that the administration of IL-17Ab attenuates this inflammatory scenario and immune response/s rescuing peripheral AD-outcome (left and right down panel).

percentage of positive cells found in the staining for the isotype control antibodies (Supplementary Fig. 12) challenged with ADP (1, 3 and 10 μM). Results are shown as % of aggregation, which reflects the maximum amplitude of the curve (Fig. 5H), and AUC, which is an expression of overall platelet activity (Fig. 5I). As expected, there was an enhanced platelet aggregation since ADP response was significantly higher in AD group compared to CTRL at all tested concentrations (Fig. 5H-I). Platelets harvested from the IL-17Ab group displayed a reduced value of AUC, but not % of aggregation, when challenged with ADP 10 μM (Fig. 5I). Both parameters were not affected by 1 and 3 μM of ADP in terms of % of aggregation (Fig. 5H) and AUC (Fig. 5I). These results confirm the presence of an activated state of platelets in this preclinical model as observed in AD. Therefore, platelets and coagulation cascades are feasible to foster each other, displaying a synergistic effect reciprocally. The finding that IL-17Ab affects the AUC but not the % of aggregation implies that IL-17 amplifies, rather than directly induces, platelet aggregation.

4. Conclusions

Alzheimer's disease (AD) is a common neurodegenerative disease characterized by a neuro-inflammatory state, and to date, its treatment represents a large unmet clinical need. The involvement of IL-17 in the pathogenesis and progression of AD-related neuro-inflammation has been reported in several studies. However, the role of this cytokine on the systemic/peripheral features of AD has not been addressed. In this study, we have demonstrated that the selected non-genetic mouse model of $A\beta_{1-42}$-induced Alzheimer's disease, not only recapitulates the neuro-inflammation typical of AD, but also provides the main systemic/peripheral features of the pathology. Indeed, this model allows simultaneous evaluation of systemic inflammation, immunological perturbance, peripheral vascular/endothelial impairment, and the prothrombotic state. In this context, we have unveiled a pivotal role of brain-derived IL-17 (mainly produced by $Th17^{+}$ cells) as a circulating trigger for the unconventional endothelium/platelets activation leading to sustaining inflammatory mechanism(s) related to AD (Fig. 6). IL-17 neutralizing antibody treatment modulates all these features suggesting novel, alternative therapeutic approaches for managing the multifaced aspects of AD.

CRediT authorship contribution statement

V.V., A.S., F.R., G.M.C., A.A.M., E.P. and E.M. performed the experiments and data analysis. G.D.F., N.F., R.d.d.V.B., R.S., A.J.I., G.C., M.B and F.M. wrote the manuscript. A.J.I., G.C., M.B. and F.M. revised the final version of the manuscript for intellectual contents. All authors gave final approval to the publication.

Conflict of interest

This article has been conducted and written in the absence of any commercial or financial relationships that could be construed as a potential conflict of interest.

Data Availability

Data will be made available on request.

Acknowledgements

This work was supported by MIUR (PRIN 202039WMFP_004). New interventional approaches on multiple inflammatory pathways involvedin regeneration after trauma and aging-associated diseases. PRIN 2017; 2017A95NCJ/2017A95NCJ_002, "Stolen molecules - Stealing natural products from the depot and reselling them as new drug candidates", and in part by PRIN 2017XZMBYX_003 "Unraveling hidden culprits for the cardiac arrhythmia burden: Modulation of immunoinflammation and inter-cellular signaling as targets for novel therapeutic approaches", and PRIN 2017B9NCSX_005, "Studies of the crosstalk between multiple pathways in the regulation of inflammatory processes in models of chronic and degenerative diseases". AJI is awarded by Birmingham Fellowship. AS is supported by Dompé farmaceutici S.p.A fellowship for PhD program in "Nutraceuticals, functional foods and human health" (University of Naples Federico II) and FR is supported by University of Naples Federico II PhD Scholarship in Pharmaceutical Sciences.

Appendix A. Supporting information

Supplementary data associated with this article can be found in the online version at doi:10.1016/j.phrs.2022.106595.

References

[1] D.R. Thal, W.S. Griffin, R.A. de Vos, E. Ghebremedhin, Cerebral amyloid angiopathy and its relationship to Alzheimer's disease, Acta Neuropathol. 115 (2008) 599–609, https://doi.org/10.1007/s00401-008-0366-2.
[2] E.E. Smith, S.M. Greenberg, Beta-amyloid, blood vessels, and brain function, Stroke 40 (2009) 2601–2606, https://doi.org/10.1161/strokeaha.108.536839.
[3] L.S. Honig, M.X. Tang, S. Albert, R. Costa, J. Luchsinger, J. Manly, Y. Stern, R. Mayeux, Stroke and the risk of Alzheimer disease, Arch. Neurol. 60 (2003) 1707–1712, https://doi.org/10.1001/archneur.60.12.1707.
[4] K. Javanshiri, M.L. Waldö, N. Friberg, F. Sjövall, K. Wickerström, M. Haglund, E. Englund, Atherosclerosis, hypertension, and diabetes in Alzheimer's disease, vascular dementia, and mixed dementia: prevalence and presentation, J. Alzheimers Dis. 65 (2018) 1247–1258, https://doi.org/10.3233/jad-180644.
[5] M.M. Mielke, P.B. Rosenberg, J. Tschanz, L. Cook, C. Corcoran, K.M. Hayden, M. Norton, P.V. Rabins, R.C. Green, K.A. Welsh-Bohmer, J.C. Breitner, R. Munger, C.G. Lyketsos, Vascular factors predict rate of progression in Alzheimer disease, Neurology 69 (2007) 1850–1858, https://doi.org/10.1212/01.wnl.0000279520.59792.fe.
[6] H.J. Ahn, D. Zamolodchikov, M. Cortes-Canteli, E.H. Norris, J.F. Glickman, S. Strickland, Alzheimer's disease peptide beta-amyloid interacts with fibrinogen and induces its oligomerization, Proc. Natl. Acad. Sci. USA 107 (2010) 21812–21817, https://doi.org/10.1073/pnas.1010373107.
[7] D. Zamolodchikov, H.E. Berk-Rauch, D.A. Oren, D.S. Stor, P.K. Singh, M. Kawasaki, K. Aso, S. Strickland, H.J. Ahn, Biochemical and structural analysis of the interaction between β-amyloid and fibrinogen, Blood 128 (2016) 1144–1151, https://doi.org/10.1182/blood-2016-03-705228.
[8] S. Strickland, Blood will out: vascular contributions to Alzheimer's disease, J. Clin. Invest 128 (2018) 556–563, https://doi.org/10.1172/jci97509.
[9] W.S. Hur, N. Mazinani, X.J.D. Lu, L.S. Yefet, J.R. Byrnes, L. Ho, J.H. Yeon, S. Filipenko, A.S. Wolberg, W.A. Jefferies, C.J. Kastrup, Coagulation factor XIIIa cross-links amyloid β into dimers and oligomers and to blood proteins, J. Biol. Chem. 294 (2019) 390–396, https://doi.org/10.1074/jbc.RA118.005352.
[10] G.L. Suidan, P.K. Singh, S. Patel-Hett, Z.L. Chen, D. Volfson, H. Yamamoto-Imoto, E.H. Norris, R.D. Bell, S. Strickland, Abnormal clotting of the intrinsic/contact pathway in Alzheimer disease patients is related to cognitive ability, Blood Adv. 2 (2018) 954–963, https://doi.org/10.1182/bloodadvances.2018017798.
[11] Y. Iturria-Medina, R.C. Sotero, P.J. Toussaint, J.M. Mateos-Pérez, A.C. Evans, Early role of vascular dysregulation on late-onset Alzheimer's disease based on multifactorial data-driven analysis, Nat. Commun. 7 (2016) 11934, https://doi.org/10.1038/ncomms11934.
[12] F.J. Wolters, H.I. Zonneveld, A. Hofman, A. van der Lugt, P.J. Koudstaal, M. W. Vernooij, M.A. Ikram, Cerebral perfusion and the risk of dementia: a population-based study, Circulation 136 (2017) 719–728, https://doi.org/10.1161/circulationaha.117.027448.
[13] M. Cortes-Canteli, L. Mattei, A.T. Richards, E.H. Norris, S. Strickland, Fibrin deposited in the Alzheimer's disease brain promotes neuronal degeneration, Neurobiol. Aging 36 (2015) 608–617, https://doi.org/10.1016/j.neurobiolaging.2014.10.030.
[14] M. Cortes-Canteli, J. Paul, E.H. Norris, R. Bronstein, H.J. Ahn, D. Zamolodchikov, S. Bhuvanendran, K.M. Fenz, S. Strickland, Fibrinogen and beta-amyloid association alters thrombosis and fibrinolysis: a possible contributing factor to Alzheimer's disease, Neuron 66 (2010) 695–709, https://doi.org/10.1016/j.neuron.2010.05.014.
[15] M. Noguchi, T. Sato, K. Nagai, I. Utagawa, I. Suzuki, M. Arito, N. Iizuka, N. Suematsu, K. Okamoto, T. Kato, N. Yamaguchi, M.S. Kurokawa, Roles of serum fibrinogen α chain-derived peptides in Alzheimer's disease, Int J. Geriatr. Psychiatry 29 (2014) 808–818, https://doi.org/10.1002/gps.4047.
[16] Y. Kitamura, R. Usami, S. Ichihara, H. Kida, M. Satoh, H. Tomimoto, M. Murata, S. Oikawa, Plasma protein profiling for potential biomarkers in the early diagnosis of Alzheimer's disease, Neurol. Res. 39 (2017) 231–238, https://doi.org/10.1080/01616412.2017.1281195.
[17] S. Sevush, W. Jy, L.L. Horstman, W.W. Mao, L. Kolodny, Y.S. Ahn, Platelet activation in Alzheimer disease, Arch. Neurol. 55 (1998) 530–536, https://doi.org/10.1001/archneur.55.4.530.

[18] C. Cristiano, F. Volpicelli, P. Lippiello, B. Buono, F. Raucci, M. Piccolo, A.J. Iqbal, C. Irace, M.C. Miniaci, C. Perrone Capano, A. Calignano, N. Mascolo, F. Maione, Neutralization of IL-17 rescues amyloid-β-induced neuroinflammation and memory impairment, Br. J. Pharm. 176 (2019) 3544–3557, https://doi.org/10.1111/bph.14586.

[19] J. Milovanovic, A. Arsenijevic, B. Stojanovic, T. Kanjevac, D. Arsenijevic, G. Radosavljevic, M. Milovanovic, N. Arsenijevic, Interleukin-17 in Chronic Inflammatory Neurological Diseases, Front Immunol. 11 (2020) 947, https://doi.org/10.3389/fimmu.2020.00947.

[20] M. Saresella, E. Calabrese, I. Marventano, F. Piancone, A. Gatti, M. Alberoni, R. Nemni, M. Clerici, Increased activity of Th-17 and Th-9 lymphocytes and a skewing of the post-thymic differentiation pathway are seen in Alzheimer's disease, Brain Behav. Immun. 25 (2011) 539–547, https://doi.org/10.1016/j.bbi.2010.12.004.

[21] J. Zhang, K.F. Ke, Z. Liu, Y.H. Qiu, Y.P. Peng, Th17 cell-mediated neuroinflammation is involved in neurodegeneration of aβ1-42-induced Alzheimer's disease model rats, PLoS One 8 (2013), e75786, https://doi.org/10.1371/journal.pone.0075786.

[22] J. Chen, X. Liu, Y. Zhong, Interleukin-17A: the key cytokine in neurodegenerative diseases, Front Aging Neurosci. 12 (2020), 566922, https://doi.org/10.3389/fnagi.2020.566922.

[23] H. Kebir, K. Kreymborg, I. Ifergan, A. Dodelet-Devillers, R. Cayrol, M. Bernard, F. Giuliani, N. Arbour, B. Becher, A. Prat, Human TH17 lymphocytes promote blood-brain barrier disruption and central nervous system inflammation, Nat. Med 13 (2007) 1173–1175, https://doi.org/10.1038/nm1651.

[24] J.M. Chen, Q.W. Li, G.X. Jiang, J.S. Liu, Q. Cheng, IL-18 induced IL-23/IL-17 expression impairs Aβ clearance in cultured THP-1 and BV2 cells, Cytokine 119 (2019) 113–118, https://doi.org/10.1016/j.cyto.2019.03.003.

[25] C. Kilkenny, W.J. Browne, I.C. Cuthill, M. Emerson, D.G. Altman, Improving bioscience research reporting: the ARRIVE guidelines for reporting animal research, J. Pharm. Pharm. 1 (2010) 94–99, https://doi.org/10.4103/0976-500x.72351.

[26] J.C. McGrath, E. Lilley, Implementing guidelines on reporting research using animals (ARRIVE etc.): new requirements for publication in BJP, Br. J. Pharm. 172 (2015) 3189–3193, https://doi.org/10.1111/bph.12955.

[27] F. Maione, M. Piccolo, S. De Vita, M.G. Chini, C. Cristiano, C. De Caro, P. Lippiello, M.C. Miniaci, R. Santamaria, C. Irace, V. De Feo, A. Calignano, N. Mascolo, G. Bifulco, Down regulation of pro-inflammatory pathways by tanshinone IIA and cryptotanshinone in a non-genetic mouse model of Alzheimer's disease, Pharm. Res 129 (2018) 482–490, https://doi.org/10.1016/j.phrs.2017.11.018.

[28] E. Mhillaj, M.G. Morgese, P. Tucci, A. Furiano, L. Luongo, M. Bove, S. Maione, V. Cuomo, S. Schiavone, L. Trabace, Celecoxib prevents cognitive impairment and neuroinflammation in soluble amyloid β-treated rats, Neuroscience 372 (2018) 58–73, https://doi.org/10.1016/j.neuroscience.2017.12.046.

[29] A. Pires, A. Fortuna, G. Alves, A. Falcão, Intranasal drug delivery: how, why and what for, J. Pharm. Pharm. Sci. 12 (2009) 288–311, https://doi.org/10.18433/j3nc79.

[30] F. Raucci, A.J. Iqbal, A. Saviano, G.M. Casillo, M. Russo, D. Lezama, N. Mascolo, F. Maione, In-depth immunophenotyping data relating to IL-17Ab modulation of circulating Treg/Th17 cells and of in situ infiltrated inflammatory monocytes in the onset of gouty inflammation, Data Brief. 25 (2019), 104381, https://doi.org/10.1016/j.dib.2019.104381.

[31] F. Maione, C. Cicala, E. Liverani, N. Mascolo, M. Perretti, F. D'Acquisto, IL-17A increases ADP-induced platelet aggregation, Biochem Biophys. Res Commun. 408 (2011) 658–662, https://doi.org/10.1016/j.bbrc.2011.04.080.

[32] F. Maione, A.J. Iqbal, F. Raucci, M. Letek, M. Bauer, F. D'Acquisto, Repetitive exposure of IL-17 into the murine air pouch favors the recruitment of inflammatory monocytes and the release of IL-16 and TREM-1 in the inflammatory fluids, Front Immunol. 9 (2018) 2752, https://doi.org/10.3389/fimmu.2018.02752.

[33] A. Cossarizza, H.D. Chang, A. Radbruch, S. Abrignani, R. Addo, M. Akdis, I. Andrä, F. Andreata, F. Annunziato, E. Arranz, P. Bacher, S. Bari, V. Barnaba, J. Barros-Martins, D. Baumjohann, C.G. Beccaria, D. Bernardo, D.A. Boardman, J. Borger, C. Böttcher, L. Brockmann, M. Burns, D.H. Busch, G. Cameron, I. Cammarata, A. Cassotta, Y. Chang, F.G. Chirdo, E. Christakou, L. Čičin-Šain, L. Cook, A. J. Corbett, R. Cornelis, L. Cosmi, M.S. Davey, S. De Biasi, G. De Simone, G. Del Zotto, M. Delacher, F. Di Rosa, J. Di Santo, A. Diefenbach, J. Dong, T. Dörner, R. J. Dress, C.A. Dutertre, S.B.G. Eckle, P. Eede, M. Evrard, C.S. Falk, M. Feuerer, S. Fillatreau, A. Fiz-Lopez, M. Follo, G.A. Foulds, J. Fröbel, N. Gagliani, G. Galletti, A. Gangaev, N. Garbi, J.A. Garrote, J. Geginat, N.A. Gherardin, L. Gibellini, F. Ginhoux, D.I. Godfrey, P. Gruarin, C. Haftmann, L. Hansmann, C.M. Harpur, A. C. Hayday, G. Heine, D.C. Hernández, M. Herrmann, O. Hoelsken, Q. Huang, S. Huber, J.E. Huber, J. Huehn, M. Hundemer, W.Y.K. Hwang, M. Iannacone, S. M. Ivison, H.M. Jäck, P.K. Jani, B. Keller, N. Kessler, S. Ketelaars, L. Knop, J. Knopf, H.F. Koay, K. Kobow, K. Kriegsmann, H. Kristyanto, A. Krueger, J.F. Kuehne, H. Kunze-Schumacher, P. Kvistborg, I. Kwok, D. Latorre, D. Lenz, M.K. Levings, A. C. Lino, F. Liotta, H.M. Long, E. Lugli, K.N. MacDonald, L. Maggi, M.K. Maini, F. Mair, C. Manta, R.A. Manz, M.F. Mashreghi, A. Mazzoni, J. McCluskey, H.E. Mei, F. Melchers, S. Melzer, D. Mielenz, L. Monin, L. Moretta, G. Multhoff, L.E. Muñoz, M. Muñoz-Ruiz, F. Muscate, A. Natalini, K. Neumann, L.G. Ng, A. Niedobitek, J. Niemz, L.N. Almeida, S. Notarbartolo, L. Ostendorf, L.J. Pallett, A.A. Patel, G. I. Percin, G. Peruzzi, M. Pinti, A.G. Pockley, K. Pracht, I. Prinz, I. Pujol-Autonell, N. Pulvirenti, L. Quatrini, K.M. Quinn, H. Radbruch, H. Rhys, M.B. Rodrigo, C. Romagnani, C. Saggau, S. Sakaguchi, F. Sallusto, L. Sanderink, I. Sandrock, C. Schauer, A. Scheffold, H.U. Scherer, M. Schiemann, F.A. Schildberg, K. Schober, J. Schoen, W. Schuh, T. Schüler, A.R. Schulz, S. Schulz, J. Schulze, S. Simonetti, J. Singh, K.M. Sitnik, R. Stark, S. Starossom, C. Stehle, F. Szelinski, L. Tan, A. Tarnok, J. Tornack, T.I.M. Tree, J.J.P. van Beek, W. van de Veen, K. van Gisbergen, C. Vasco, N.A. Verheyden, A. von Borstel, K.A. Ward-Hartstonge, K. Warnatz, C. Waskow, A. Wiedemann, A. Wilharm, J. Wing, O. Wirz, J. Wittner, J.H.M. Yang, J. Yang, Guidelines for the use of flow cytometry and cell sorting in immunological studies (third edition, Eur. J. Immunol. 51 (2021) 2708–3145, doi: 10.1002/eji.202170126.

[34] A. Saviano, F. Raucci, G.M. Casillo, A.A. Mansour, V. Piccolo, C. Montesano, M. Smimmo, V. Vellecco, G. Capasso, A. Boscaino, V. Summa, N. Mascolo, A. J. Iqbal, R. Sorrentino, R. d'Emmanuele di Villa Bianca, M. Bucci, V. Brancaleone, F. Maione, Anti-inflammatory and immunomodulatory activity of Mangifera indica L. reveals the modulation of COX-2/mPGES-1 axis and Th17/Treg ratio, Pharm. Res 182 (2022), 106283, https://doi.org/10.1016/j.phrs.2022.106283.

[35] Q. Gao, Y. Wang, X. Wang, S. Fu, X. Zhang, R.T. Wang, X. Zhang, Decreased levels of circulating trimethylamine N-oxide alleviate cognitive and pathological deterioration in transgenic mice: a potential therapeutic approach for Alzheimer's disease, Aging (Albany NY) 11 (2019) 8642–8663, https://doi.org/10.18632/aging.102352.

[36] E. Tarkowski, A. Wallin, B. Regland, K. Blennow, A. Tarkowski, Local and systemic GM-CSF increase in Alzheimer's disease and vascular dementia, Acta Neurol. Scand. 103 (2001) 166–174, https://doi.org/10.1034/j.1600-0404.2001.103003166.x.

[37] J. Kipnis, M. Cardon, H. Avidan, G.M. Lewitus, S. Mordechay, A. Rolls, Y. Shani, M. Schwartz, Dopamine, through the extracellular signal-regulated kinase pathway, downregulates CD4+CD25+ regulatory T-cell activity: implications for neurodegeneration, J. Neurosci. 24 (2004) 6133–6143, https://doi.org/10.1523/jneurosci.0600-04.2004.

[38] A.A. Mamchak, Y. Manenkova, W. Leconet, Y. Zheng, J.R. Chan, C.L. Stokes, L. K. Shoda, M. von Herrath, D. Bresson, Preexisting autoantibodies predict efficacy of oral insulin to cure autoimmune diabetes in combination with anti-CD3, Diabetes 61 (2012) 1490–1499, https://doi.org/10.2337/db11-1304.

[39] F. Raucci, A.J. Iqbal, A. Saviano, P. Minosi, M. Piccolo, C. Irace, F. Caso, R. Scarpa, S. Pieretti, N. Mascolo, F. Maione, IL-17A neutralizing antibody regulates monosodium urate crystal-induced gouty inflammation, Pharm. Res. 147 (2019), 104351, https://doi.org/10.1016/j.phrs.2019.104351.

[40] A. Saviano, G.M. Casillo, F. Raucci, A. Pernice, C. Santarcangelo, M. Piccolo, M. G. Ferraro, M. Ciccone, A. Sgherbini, N. Pedretti, D. Bonvicini, C. Irace, M. Daglia, N. Mascolo, F. Maione, Supplementation with ribonucleotide-based ingredient (Ribodiet®) lessens oxidative stress, brain inflammation, and amyloid pathology in a murine model of Alzheimer, Biomed. Pharm. 139 (2021), 111579, https://doi.org/10.1016/j.biopha.2021.111579.

[41] F. Raucci, A. Saviano, G.M. Casillo, M. Guerra-Rodriguez, A.A. Mansour, M. Piccolo, M.G. Ferraro, E. Panza, V. Vellecco, C. Irace, F. Caso, R. Scarpa, N. Mascolo, M. Alfaifi, A.J. Iqbal, F. Maione, IL-17-induced inflammation modulates the mPGES-1/PPAR-γ pathway in monocytes/macrophages, 10.1111/bph.15413, Br. J. Pharmacol. (2021), https://doi.org/10.1111/bph.15413.

[42] K. Yamade, T. Yamaguchi, Y. Nagai, T. Kamisako, Platelet count evaluation compared with the immunoplatelet reference method and performance evaluation of the hematology analyzer Celltac G, Int. J. Lab Hematol. 43 (2021) 927–938, https://doi.org/10.1111/ijlh.13481.

[43] L. Di Cesare Mannelli, M. Piccolo, F. Maione, M.G. Ferraro, C. Irace, V. De Feo, C. Ghelardini, N. Mascolo, Tanshinones from Salvia miltiorrhiza Bunge revert chemotherapy-induced neuropathic pain and reduce glioblastoma cells malignancy, Biomed. Pharm. 105 (2018) 1042–1049, https://doi.org/10.1016/j.biopha.2018.06.047.

[44] D.A. Law, F.R. DeGuzman, P. Heiser, K. Ministri-Madrid, N. Killeen, D.R. Phillips, Integrin cytoplasmic tyrosine motif is required for outside-in alphaIIbbeta3 signalling and platelet function, Nature 401 (1999) 808–811, https://doi.org/10.1038/44599.

[45] K.L. Tucker, T. Sage, J.M. Gibbins, Clot retraction, Methods Mol. Biol. 788 (2012) 101–107, https://doi.org/10.1007/978-1-61779-307-3_8.

[46] A.C. Pearce, P. Wonerow, S.J. Marshall, J. Frampton, T.K. Gartner, S.P. Watson, The heptapeptide LSARLAF mediates platelet activation through phospholipase Cgamma2 independently of glycoprotein IIb-IIIa, Biochem. J. 378 (2004) 193–199, https://doi.org/10.1042/bj20031298.

[47] V. Mirone, R. d'Emmanuele di Villa Bianca, E. Mitidieri, C. Imbimbo, F. Fusco, P. Verze, D.F. Vitale, R. Sorrentino, G. Cirino, Platelet cyclic guanosine monophosphate as a biomarker of phosphodiesterase type 5 inhibitor efficacy in the treatment of erectile dysfunction: a randomized placebo-controlled study, Eur. Urol. 56 (2009) 1067–1073, https://doi.org/10.1016/j.eururo.2009.09.031.

[48] V. Vellecco, E. Mitidieri, A. Gargiulo, V. Brancaleone, D. Matassa, T. Klein, F. Esposito, G. Cirino, M. Bucci, Vascular effects of linagliptin in non-obese diabetic mice are glucose-independent and involve positive modulation of the endothelial nitric oxide synthase (eNOS)/caveolin-1 (CAV-1) pathway, Diabetes Obes. Metab. 18 (2016) 1236–1243, https://doi.org/10.1111/dom.12750.

[49] E. Mitidieri, T. Tramontano, D. Gurgone, V. Citi, V. Calderone, V. Brancaleone, A. Katsouda, N. Nagahara, A. Papapetropoulos, G. Cirino, R. d'Emmanuele di Villa Bianca, R. Sorrentino, Mercaptopyruvate acts as endogenous vasodilator independently of 3-mercaptopyruvate sulfurtransferase activity, Nitric Oxide 75 (2018) 53–59, https://doi.org/10.1016/j.niox.2018.02.003.

[50] A. Rauf, M. Saleem, G. Uddin, B.S. Siddiqui, H. Khan, M. Raza, S.Z. Hamid, A. Khan, F. Maione, N. Mascolo, V. De Feo, Phosphodiesterase-1 Inhibitory Activity of Two Flavonoids Isolated from Pistacia integerrima J. L. Stewart Galls, Evid. Based Complement Altern. Med 2015 (2015), 506564, https://doi.org/10.1155/2015/506564.

[51] G. Yetik-Anacak, A. Dikmen, C. Coletta, E. Mitidieri, M. Dereli, E. Donnarumma, R. d'Emmanuele di Villa Bianca, R. Sorrentino, Hydrogen sulfide compensates

nitric oxide deficiency in murine corpus cavernosum, Pharm. Res 113 (2016) 38–43, https://doi.org/10.1016/j.phrs.2016.08.015.
[52] E. Panza, V. Vellecco, F.A. Iannotti, D. Paris, O.L. Manzo, M. Smimmo, N. Mitilini, A. Boscaino, G. de Dominicis, M. Bucci, A. Di Lorenzo, G. Cirino, Duchenne's muscular dystrophy involves a defective transsulfuration pathway activity, Redox Biol. 45 (2021), 102040, https://doi.org/10.1016/j.redox.2021.102040.
[53] F. Maione, N. Paschalidis, N. Mascolo, N. Dufton, M. Perretti, F. D'Acquisto, Interleukin 17 sustains rather than induces inflammation, Biochem Pharm. 77 (2009) 878–887, https://doi.org/10.1016/j.bcp.2008.11.011.
[54] M.J. Curtis, S. Alexander, G. Cirino, J.R. Docherty, C.H. George, M.A. Giembycz, D. Hoyer, P.A. Insel, A.A. Izzo, Y. Ji, D.J. MacEwan, C.G. Sobey, S.C. Stanford, M. M. Teixeira, S. Wonnacott, A. Ahluwalia, Experimental design and analysis and their reporting II: updated and simplified guidance for authors and peer reviewers, Br. J. Pharm. 175 (2018) 987–993, https://doi.org/10.1111/bph.14153.
[55] C.H. George, S.C. Stanford, S. Alexander, G. Cirino, J.R. Docherty, M.A. Giembycz, D. Hoyer, P.A. Insel, A.A. Izzo, Y. Ji, D.J. MacEwan, C.G. Sobey, S. Wonnacott, A. Ahluwalia, Updating the guidelines for data transparency in the British Journal of Pharmacology - data sharing and the use of scatter plots instead of bar charts, Br. J. Pharmacol. 174 (2017) 2801–2804, https://doi.org/10.1111/bph.13925.
[56] S.P.H. Alexander, R.E. Roberts, B.R.S. Broughton, C.G. Sobey, C.H. George, S. C. Stanford, G. Cirino, J.R. Docherty, M.A. Giembycz, D. Hoyer, P.A. Insel, A. A. Izzo, Y. Ji, D.J. MacEwan, J. Mangum, S. Wonnacott, A. Ahluwalia, Goals and practicalities of immunoblotting and immunohistochemistry: a guide for submission to the British Journal of Pharmacology, Br. J. Pharmacol. 175 (2018) 407–411, https://doi.org/10.1111/bph.14112.
[57] S.M. Cho, H.V. Kim, S. Lee, H.Y. Kim, W. Kim, T.S. Kim, D.J. Kim, Y. Kim, Correlations of amyloid-β concentrations between CSF and plasma in acute Alzheimer mouse model, Sci. Rep. 4 (2014) 6777, https://doi.org/10.1038/srep06777.
[58] M. Cortes-Canteli, C. Iadecola, Alzheimer's disease and vascular aging: JACC focus seminar, J. Am. Coll. Cardiol. 75 (2020) 942–951, https://doi.org/10.1016/j.jacc.2019.10.062.
[59] E. Paouri, S. Georgopoulos, Systemic and CNS inflammation crosstalk: implications for Alzheimer's disease, Curr. Alzheimer Res 16 (2019) 559–574, https://doi.org/10.2174/1567205016666190321154618.
[60] I.M. Rea, D.S. Gibson, V. McGilligan, S.E. McNerlan, H.D. Alexander, O.A. Ross, Age and age-related diseases: role of inflammation triggers and cytokines, Front Immunol. 9 (2018) 586, https://doi.org/10.3389/fimmu.2018.00586.
[61] C.R. Jack Jr., D.A. Bennett, K. Blennow, M.C. Carrillo, B. Dunn, S.B. Haeberlein, D. M. Holtzman, W. Jagust, F. Jessen, J. Karlawish, E. Liu, J.L. Molinuevo, T. Montine, C. Phelps, K.P. Rankin, C.C. Rowe, P. Scheltens, E. Siemers, H.M. Snyder, R. Sperling, NIA-AA Research Framework: Toward a biological definition of Alzheimer's disease, Alzheimers Dement 14 (2018) 535–562, https://doi.org/10.1016/j.jalz.2018.02.018.
[62] J.M. Rubio-Perez, J.M. Morillas-Ruiz, A review: inflammatory process in Alzheimer's disease, role of cytokines, Sci. World J. 2012 (2012), 756357, https://doi.org/10.1100/2012/756357.
[63] A.H. van den Biggelaar, J. Gussekloo, A.J. de Craen, M. Frölich, M.L. Stek, R.C. van der Mast, R.G. Westendorp, Inflammation and interleukin-1 signaling network contribute to depressive symptoms but not cognitive decline in old age, Exp. Gerontol. 42 (2007) 693–701, https://doi.org/10.1016/j.exger.2007.01.011.
[64] C. Holmes, C. Cunningham, E. Zotova, D. Culliford, V.H. Perry, Proinflammatory cytokines, sickness behavior, and Alzheimer disease, Neurology 77 (2011) 212–218, https://doi.org/10.1212/WNL.0b013e318225ae07.
[65] J.R. Hall, L.A. Johnson, R.C. Barber, H.T. Vo, A.S. Winter, S.E. O'Bryant, Biomarkers of basic activities of daily living in Alzheimer's disease, J. Alzheimers Dis. 31 (2012) 429–437, https://doi.org/10.3233/jad-2012-111481.
[66] M. Rentzos, A. Rombos, The role of IL-15 in central nervous system disorders, Acta Neurol. Scand. 125 (2012) 77–82, https://doi.org/10.1111/j.1600-0404.2011.01524.x.
[67] P. Bossù, A. Ciaramella, F. Salani, F. Bizzoni, E. Varsi, F. Di Iulio, F. Giubilei, W. Gianni, A. Trequattrini, M.L. Moro, S. Bernardini, C. Caltagirone, G. Spalletta, Interleukin-18 produced by peripheral blood cells is increased in Alzheimer's disease and correlates with cognitive impairment, Brain Behav. Immun. 22 (2008) 487–492, https://doi.org/10.1016/j.bbi.2007.10.001.
[68] K. Baruch, N. Rosenzweig, A. Kertser, A. Deczkowska, A.M. Sharif, A. Spinrad, A. Tsitsou-Kampeli, A. Sarel, L. Cahalon, M. Schwartz, Breaking immune tolerance by targeting Foxp3(+) regulatory T cells mitigates Alzheimer's disease pathology, Nat. Commun. 6 (2015) 7967, https://doi.org/10.1038/ncomms8967.
[69] Y. Yang, Z. He, Z. Xing, Z. Zuo, L. Yuan, Y. Wu, M. Jiang, F. Qi, Z. Yao, Influenza vaccination in early Alzheimer's disease rescues amyloidosis and ameliorates cognitive deficits in APP/PS1 mice by inhibiting regulatory T cells, J. Neuroinflamm. 17 (2020) 65, https://doi.org/10.1186/s12974-020-01741-4.
[70] J. Ye, Y. Wang, Z. Wang, Q. Ji, Y. Huang, T. Zeng, H. Hu, D. Ye, J. Wan, Y. Lin, Circulating Th1, Th2, Th9, Th17, Th22, and treg levels in aortic dissection patients, Mediat. Inflamm. 2018 (2018) 5697149, https://doi.org/10.1155/2018/5697149.
[71] W.C. Sessa, eNOS at a glance, J. Cell Sci. 117 (2004) 2427–2429, https://doi.org/10.1242/jcs.01165.
[72] Y. Akimoto, T. Horinouchi, M. Shibano, M. Matsushita, Y. Yamashita, T. Okamoto, F. Yamaki, Y. Tanaka, K. Koike, Nitric oxide (NO) primarily accounts for endothelium-dependent component of beta-adrenoceptor-activated smooth muscle relaxation of mouse aorta in response to isoprenaline, J. Smooth Muscle Res. 38 (2002) 87–99, https://doi.org/10.1540/jsmr.38.87.
[73] S. Banquet, E. Delannoy, A. Agouni, C. Dessy, S. Lacomme, F. Hubert, V. Richard, B. Muller, V. Leblais, Role of G(i/o)-Src kinase-PI3K/Akt pathway and caveolin-1 in β_2-adrenoceptor coupling to endothelial NO synthase in mouse pulmonary artery, Cell Signal 23 (2011) 1136–1143, https://doi.org/10.1016/j.cellsig.2011.02.008.
[74] C. Cicala, G. Cirino, Linkage between inflammation and coagulation: an update on the molecular basis of the crosstalk, Life Sci. 62 (1998) 1817–1824, https://doi.org/10.1016/s0024-3205(97)01167-3.
[75] M. Cortes-Canteli, D. Zamolodchikov, H.J. Ahn, S. Strickland, E.H. Norris, Fibrinogen and altered hemostasis in Alzheimer's disease, J. Alzheimers Dis. 32 (2012) 599–608, https://doi.org/10.3233/jad-2012-120820.
[76] L. Donner, T. Feige, C. Freiburg, L.M. Toska, A.S. Reichert, M. Chatterjee, M. Elvers, Impact of Amyloid-β on platelet mitochondrial function and platelet-mediated amyloid aggregation in Alzheimer's disease, Int J. Mol. Sci. 22 (2021), https://doi.org/10.3390/ijms22179633.